

**UNCLASSIFIED**

**AD**

**405 937**

**DEFENSE DOCUMENTATION CENTER**

**FOR**

**SCIENTIFIC AND TECHNICAL INFORMATION**

**CAMERON STATION, ALEXANDRIA, VIRGINIA**



**UNCLASSIFIED**

NOTICE: When government or other drawings, specifications or other data are used for any purpose other than in connection with a definitely related government procurement operation, the U. S. Government thereby incurs no responsibility, nor any obligation whatsoever; and the fact that the Government may have formulated, furnished, or in any way supplied the said drawings, specifications, or other data is not to be regarded by implication or otherwise as in any manner licensing the holder or any other person or corporation, or conveying any rights or permission to manufacture, use or sell any patented invention that may in any way be related thereto.

SSD-TDR-63-109

63-36

REPORT NO.  
TDR-169(3230-12)TN-7

~~405937~~

405937

①

*Handwritten signature*

# Nonequilibrium Electron Temperature Effects in Weakly Ionized Stagnation Boundary Layers

AD NO. **FILE COPY**

20 MAY 1963

Prepared by PAUL M. CHUNG and JAMES F. MULLEN  
*Aerodynamics and Propulsion Research Laboratory*

Prepared for COMMANDER SPACE SYSTEMS DIVISION  
UNITED STATES AIR FORCE  
*Inglewood, California*

**405 937**

DDC  
JUN 11 1963  
TISIA A



LABORATORIES DIVISION • AEROSPACE CORPORATION  
CONTRACT NO. AF 04(695)-169

7.1.0

(18) (19) (4) 7.60 (5) 17505  
SSD TDR 63/109 (7) (8) (9) NA  
(12) 72p. (13) NA  
(16) (17) NA

(14) Report No.  
TDR/169/3230/12/TN/7  
~~7~~ ~~7~~ ~~7~~ ~~7~~

(6) NONEQUILIBRIUM ELECTRON TEMPERATURE EFFECTS IN  
WEAKLY IONIZED STAGNATION BOUNDARY LAYERS,

(20) W  
(21) NA  
fd

(10) Prepared by  
Paul M. Chung and James F. Mullen  
Aerodynamics and Propulsion Research Laboratory

AEROSPACE CORPORATION  
El Segundo, California

(15) -  
Contract ~~NA~~ AF 04(695) 169  
~~7~~ ~~7~~

(11) 20 May 63

Prepared for  
COMMANDER SPACE SYSTEMS DIVISION  
UNITED STATES AIR FORCE  
Inglewood, California

ABSTRACT

~~7~~  
An electron energy equation is formulated for weakly ionized stagnation boundary layers (degree of ionization in the order of 0.1 <sup>of</sup> percent or less) over highly cooled surfaces. Only the cases of moderately negative wall potential with respect to the plasma, where the ratio of the electron to ion current densities is between about ~~10~~ <sup>1/10</sup> to 10, are considered. The equation is simplified by taking advantage of the fact that the electron energy equation is rather insensitive to the detailed variation of the electron concentration profile. A solution of the simplified electron energy equation is obtained analytically for the cases where the electron temperatures are not in equilibrium with the neutral gas temperatures. The effects of nonequilibrium electron temperatures on the electrical characteristics of the boundary layer are then analyzed.

~~It was found that the equilibration process of the electron temperatures to the neutral gas temperatures is controlled by the ratio of the characteristic electron energy conduction time to the characteristic temperature equilibration time. The characteristic residence time of electrons has been conventionally used instead of the conduction time.~~

~~The ion current is found to be dependent on the electron temperature but practically independent of the potential.~~

#### ACKNOWLEDGMENT

The authors wish to acknowledge the assistance of Mr. James Holt of Aerospace Corporation who substantially improved the digital computer program for the sheath region used by P. Chung in Ref. 2.

## CONTENTS

I.	INTRODUCTION .....	1
II.	FORMULATION OF THE PROBLEM .....	3
	A.    Governing Equations .....	3
	B.    Boundary Conditions .....	5
III.	ANALYSIS OF ELECTRON ENERGY EQUATION .....	9
IV.	ELECTRICAL CHARACTERISTICS OF BOUNDARY LAYER. ....	19
V.	DISCUSSION .....	25
VI.	RANGE IN WHICH THE THEORY IS VALID. ....	35
	A.    Conservation and Poisson Equations .....	35
	B.    Electron Energy Equation .....	37
	C.    Wall Boundary Conditions .....	39
VII.	CONCLUDING REMARKS .....	43
	NOMENCLATURE .....	47
	APPENDIX A. ....	51
	APPENDIX B. ....	61
	REFERENCES .....	71

## FIGURES

1	Flow Model . . . . .	3
2	Approximate $h$ , $m_e$ and $\rho_s/\rho$ Profiles . . . . .	13
3	Nonequilibrium Electron Temperature Profiles for $Pr_e = 10^{-3}$ . . . . .	16
4	Typical Sheath Solution . . . . .	22
5a	Typical Electron, Ion, and Electric Field Distribution in Boundary Layer . . . . .	23
5b	Typical Electron, Ion, and Electric Field Distribution in Sheath Region . . . . .	23
6	Floating Potential and Ion Current versus Equilibration Parameter . . . . .	29
7	Floating Potential and Ion Current versus Plasma Flow Parameter . . . . .	30
8	Potential Across Boundary Layer and Ion Current versus Current Ratio . . . . .	31

## TABLE

1	Electrical Sheath Characteristics . . . . .	45
---	---	----



## I. INTRODUCTION

The gases surrounding hypersonic vehicles at orbital velocities and in many present-day high temperature experimental facilities are frequently ionized up to about 0.1 percent. An understanding of the electrical as well as thermal interactions between such weakly ionized gases and a solid boundary is important in the study of microwave-plasma interactions and in connection with the electro-chemical diagnostics in experimental facilities.

The electrical characteristics of the aerodynamically important stagnation region in weakly ionized gases have been previously studied by Talbot (Ref. 1) and Chung (Ref. 2). Talbot analyzed the regime where electrical sheath phenomena are pronounced in a range smaller than the mean free path of the gas, whereas Chung considered the case where electrical sheath effects are important in a range much greater than a mean free path. From both these analyses, it is clear that the electron temperature is an important factor influencing the electrical interaction. Although it is well-known that the electron temperature in the boundary layer may not be in equilibrium with the ion and neutral gas temperature, no analysis of the nonequilibrium electron temperature profile is available in the literature.

In the present study, the governing equation for the nonequilibrium electron temperature profile is formulated for the stagnation boundary layer flow of a weakly ionized gas. With some simplifying approximations this equation is solved essentially analytically for the case where there is no gas-phase recombination of electrons and ions, i. e. , the gas phase recombination of electrons and ions is frozen. It is shown that the gas-phase recombination is likely to be frozen in many practical cases, and it may be seen from the solution that a moderate rate of radiative recombination does not affect the electron temperature profiles.

The analysis is restricted to cases where the gas density is high enough to permit a boundary layer approach and the electrical sheath effects are pronounced over a range greater than a mean free path. The method presented by Chung (Ref. 2) will therefore be used to study the electrical interaction between the ionized boundary layer and the solid wall for the case of nonequilibrium electron temperature profiles.

## II. FORMULATION OF THE PROBLEM

The governing equations and boundary conditions for a highly cooled, stagnation boundary layer flow of weakly and singly ionized gas will first be formulated. The flow model is illustrated in Fig. 1.

### A. GOVERNING EQUATIONS

When the degree of ionization is much below  $\sim 1$  percent (in the order of 0.1 percent or less), neutral gas flow is practically unaffected by the charged particles present since the neutral-charged particle collisions are rare compared to the neutral-neutral particle collisions. Thus the equations governing the electrical behavior of the weakly ionized gases can be decoupled from those governing the neutral gas flow. The solutions of the latter equations are well-known for highly cooled stagnation boundary layers and will not be repeated here. In addition, since the molecular weights of the ions and neutral gas particles are of the same order of magnitude, the ion temperature will be assumed to be equal to the neutral gas temperature and, therefore, known in the present analysis.

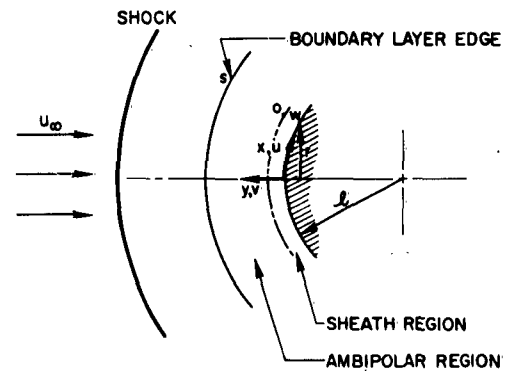


Figure 1. Flow Model

The governing equations for the electrical characteristics for two dimensional and axisymmetric stagnation boundary layers with frozen gas-phase electron-ion recombination are as follows:

#### Conservation of Ions

$$\rho u \frac{\partial C_i}{\partial x} + \rho v \frac{\partial C_i}{\partial y} = \frac{\partial}{\partial y} \left( \rho D_i \frac{\partial C_i}{\partial y} - \rho K_i E^* C_i \right) \quad (1)$$

### Conservation of Electrons

$$\rho u \frac{\partial C_e}{\partial x} + \rho v \frac{\partial C_e}{\partial y} = \frac{\partial}{\partial y} \left( \rho D_e \frac{\partial C_e}{\partial y} + \rho K_e E^* C_e \right) \quad (2)$$

### Poisson Equation

$$\frac{\partial E^*}{\partial y} = e\rho \left( \frac{C_i}{M_i} - \frac{C_e}{M_e} \right) \quad (3)$$

### Electron Energy

$$\begin{aligned} \rho u \frac{\partial (C_e c_{pe} T_e)}{\partial x} + \rho v \frac{\partial (C_e c_{pe} T_e)}{\partial y} = W_{el} - e j_e E^* \\ + \frac{\partial}{\partial y} \left[ \lambda_e \frac{\partial T_e}{\partial y} + c_{pe} T_e \left( \rho D_e \frac{\partial C_e}{\partial y} + \rho K_e E^* C_e \right) \right] \end{aligned} \quad (4)$$

where

$$c_{pe} = \frac{5}{2} \frac{k}{M_e} \quad (5)$$

The first three equations were previously derived in Ref. 2. The quantities  $W_{el}$  and  $e j_e E^*$  in the energy equation are energy source terms due to elastic collisions between the electrons and other particles and due to the electric field, respectively. The term  $c_{pe} T_e [\rho D_e (\partial C_e / \partial y) + \rho K_e E^* C_e]$  represents the electron energy transfer due to the drift of electrons. The term  $\lambda_e (\partial T_e / \partial y)$  represents the transfer of electron energy by conduction. This equation will be discussed in greater detail in subsequent sections.

With the solutions of the flow and neutral gas energy equations available, these four equations remain to determine the unknown functions  $C_i$ ,  $C_e$ ,  $E^*$ , and  $T_e$ . The equations are nonlinear and basically coupled since  $D_e$  and  $K_e$  are functions of  $T_e$ , and  $\lambda_e$ ,  $W_{el}$  and  $j_e$  depend on  $C_e$ .

#### B. BOUNDARY CONDITIONS

The plasma at  $y \rightarrow \infty$  is assumed to be neutral and to have a given charged particle concentration. In addition, though it is not necessary, the electron temperature is assumed to be equal to the neutral gas temperature there.

The boundary conditions at  $y \rightarrow \infty$  are then:

$$C_i = C_{is} \quad (6)$$

$$C_e = \frac{M_e}{M_i} C_{is} \quad (7)$$

$$T_e = T_s \quad (8)$$

Now, consider the gas-solid interface. Here the gas layer is composed of ions, electrons, and neutral gas particles in contact with the solid surface. On arrival at the interface from the boundary layer, the ions and electrons recombine catalytically, with the wall itself acting as the catalyst. If the surface is highly cooled and catalytic for electron-ion recombination, the normalized electron and ion concentrations at the interface,  $C_{ew}/C_{es}$  and  $C_{iw}/C_{is}$ , are of the order of  $(\hat{\lambda}_{gw}/\delta)$  or less<sup>1</sup>, where  $\hat{\lambda}_g$  and  $\delta$  are the neutral gas mean free path and the boundary layer thickness, respectively. For all practical purposes, therefore, the following wall boundary conditions

<sup>1</sup>This will be shown in Sec. VI.

can be used for the conservation equations when the surface is highly cooled and catalytic:

At  $y = 0$ ,

$$\frac{C_i}{C_{is}} = 0 \quad (9)$$

$$\frac{C_e}{C_{es}} = 0 \quad (10)$$

It can also be shown (Sec. VI) that for such surfaces the following boundary condition is applicable for the electron energy equation:

At  $y = 0$ ,

$$\frac{\partial T_e}{\partial y} = 0 \quad (11)$$

Boundary condition (11) implies that the temperature of the electrons at the interface will usually be different from the surface temperature. Thus, a sort of "electron temperature jump" exists at the surface. A similar phenomenon occurs in rarefied gas flow with regard to the temperature of the gas adjacent to the surface.

The temperature jump becomes negligible when  $(C_{ew}/C_{es}) > 10^{-2}$ , approximately. Such will be the case if either the surface is a poor catalyst for the electron-ion recombination or the surface temperature is much higher than  $1000^\circ\text{K}$  and has a very low work function for thermionic emission at the same time.

Finally, Poisson's equation is first order and satisfies only one boundary condition. When the surface is an electrically floating conductor or a dielectric, the boundary condition  $(j_e/j_i)_w = 1$  can be applied to the system rather

than specifying  $E^*$  at any point. The solution in this case will give  $E^* = 0$  at the boundary layer edge and an  $E^*$  corresponding to the Langmuir (floating) potential at the surface. When a net current is flowing, one may give a value of  $E^*$  or  $(j_e/j_i)_w \neq 1$  at the surface. In this case the solution gives non-vanishing  $E^*$  at the boundary layer edge. In Ref. 2 it was stated that  $E^*$  vanishes at the edge of the boundary layer. This statement must be qualified because  $E^*$  vanishes identically only when  $E_w^*$  is that value corresponding to  $(j_e/j_i)_w = 1$ . The value of  $E_s$  and its effect on the potential drop will be subsequently discussed.

### III. ANALYSIS OF ELECTRON ENERGY EQUATION

Before actually analyzing the electron energy equation, we should mention that, due to the considerable uncertainties involved in evaluating the basic physical properties of a plasma, it is not our intention to obtain detailed numerical solutions but rather to derive an approximate but essentially analytical solution, permitting the study of the effects of the major parameters.

As explained in Sec. IIA, the governing equations [Eqs. (1) through (4)] are basically coupled. Although it is clear from the Couette flow analysis of Ref. 2 that the solutions of the first three equations depend critically on the electron temperatures, the solution of the electron energy equation is rather insensitive to the detailed variation of the electron concentration profile. The latter fact will be substantiated in Sec. V. In order to simplify the analysis, therefore, the electron concentration profile is considered to be given by that obtained from the ambipolar solution of the conservation equations [Eqs. (1) and (2)] all the way to the wall. From the analysis in Ref. 2, it can be seen that such an approximation is quite acceptable for the present cases where the sheath is much thinner than the boundary layer. This approximation decouples the electron energy equation from the conservation and Poisson equations, and the analysis of the electron energy equation is simplified considerably. After the electron temperature profiles are obtained, the electrical characteristics of the boundary layer will be studied by solving the conservation and Poisson equations using a procedure similar to that in Ref. 2, with the electron temperature profiles found by the method described above.

An outline leading to the solution of the electron energy equation is given in the remainder of this section. The details of the method of solution are given in Appendix A.



The present analysis is limited to the regime in which  $10^{-1} \leq (j_e/j_i)_w \leq 10$  and  $(T_e/T_g) \leq 10$ . The former implies stagnation surfaces whose potential with respect to the plasma is weakly or moderately negative. The latter follows from the already stated condition of  $T_{es} = T_s$ . (Because  $T_s/T_w$  is in the order of 10 for the highly cooled walls, the maximum ratio of  $T_e/T_g$  will also be of the order of 10.) In this regime, the electron energy equation is simplified substantially by observing the fact that the energy source term  $e j_e E^*$  and the electron energy transfer term due to the electron drift  $c_{pe} T_e [\rho D_e (\partial C_e / \partial y) + \rho K_e E^* C_e]$  are negligible compared to the electron energy conduction term.

The electron thermal conductivity  $\lambda_e$  is obtained from Fay (Ref. 3). The expression for the energy source term  $W_{el}$  is derived from the basic equation given by Petchek and Byron (Ref. 4) with a proper consideration of the fact that the predominant elastic collision in the present problem is between the electrons and the neutral particles rather than between the electrons and the ions as is the case in Ref. 4.

The electron energy equation, Eq. (4), is thus simplified and becomes

$$\theta'' + \left( \frac{m'_e}{m_e} + \text{Pr}_e f \right) \theta' = -\text{Pr}_e \Gamma_{el} \left( \frac{\rho}{\rho_s} \right) (h - \theta) \quad (12)$$

after the usual similarity transformation, where ,

$$\text{Pr}_e = \frac{\text{Pr}_g}{2^{3/2}} \sqrt{\frac{M_e}{M_g}} \quad (13)$$

$$\Gamma_{el} = \frac{1}{1 + \epsilon} \frac{12\sqrt{3}}{5} \frac{\gamma_{eg} p_s}{T_s \sqrt{k M_e}} \left( \frac{M_e}{M_g} \right)^{1/2} \quad (14)$$

and (') denotes the differentiation with respect to the similarity variable  $\eta$ . For most gases,  $Pr_e$  is of the order of  $10^{-3}$ . The stream function  $f$  is tabulated in Ref. 5. When the collision cross section between the electrons and the air neutral particles given by Hansen (Ref. 6) is used, Eq. (14) becomes

$$\Gamma_{el} \approx \frac{1}{1 + \epsilon} 2 \times 10^{10} \frac{p_s}{T_s \beta} \quad (15)$$

where  $p_s$  is in atmospheres,  $T_s$  is in  $^{\circ}K$ , and  $\beta$  is in  $sec^{-1}$ .  $\Gamma_{el}$  denotes the ratio of the characteristic convection time (represented by  $1/\beta$ ) to the characteristic equilibration time between the electron and the neutral gas temperatures (represented by the remainder of the terms in this parameter). On the other hand, the term  $Pr_e$  denotes the ratio of characteristic conduction time to characteristic convection time for the electron thermal energy. It is seen that for given  $h(\eta)$  and  $m_e(\eta)$ , the solution of the electron energy equation depends on the two parameters  $Pr_e$  and  $\Gamma_{el}$ . For a given  $Pr_e$ ,  $\Gamma_{el} \rightarrow 0$  implies that the temperature equilibration process is frozen compared to the convection process, whereas  $\Gamma_{el} \rightarrow \infty$  implies that the electron temperatures are in equilibrium with the neutral gas temperatures.

To solve Eq. (12) analytically, the electron energy boundary layer is divided into three regions as shown in Fig. 2. The  $h$  and  $m_e$  profiles are each replaced by linear profiles. The quantity  $\rho_s/\rho$  appearing on the right-hand side of Eq. (12) follows  $m_e$  instead of  $h$  in region 2 and is  $\rho_w/\rho_s$  in region 1. The values of  $\eta_{mm}$  and  $\eta_m$  that divide the three regions are given by Eq. (25). The replacement of boundary layer profiles by linear profiles is a quite common practice, and the  $m_e$  and  $h$  profiles differ very little when  $Sc_a$  is of the order of  $Pr_g$ . These approximations, therefore, should not lead to large errors in the results. The solutions of Eq. (12) for the three regions

respectively are obtained analytically and satisfy the boundary conditions  $\theta'_w = 0$  and  $\theta_s = 1$ . The results are:

For region 1 ( $0 \leq \eta \leq \eta_{mm}$ )

$$\begin{aligned}
 \theta(\rho_1) = & \gamma_1 I_0 + \left[ \left( h_w - \frac{h'_w}{m'_{ew}} m_{ew} \right) (\rho_1 K_1) \right. \\
 & + \left. \left( h'_w \sqrt{\frac{h_w}{Pr_e \Gamma_{el}}} \right) \left( \rho_1^2 K_1 + \rho_1 K_0 - \int_{\rho_{1w}}^{\rho_1} K_0 d\rho_1 \right) \right] I_0 \\
 & + \left[ \left( h_w - \frac{h'_w}{m'_{ew}} m_{ew} \right) (\rho_1 I_1) \right. \\
 & + \left. \left( h'_w \sqrt{\frac{h_w}{Pr_e \Gamma_{el}}} \right) \left( \rho_1^2 I_1 - \rho_1 I_0 + \int_{\rho_{1w}}^{\rho_1} I_0 d\rho_1 \right) \right] K_0
 \end{aligned} \tag{16}$$

where

$$\rho_1 = \sqrt{\frac{Pr_e \Gamma_{el}}{h_w} \left( \frac{m_{ew}}{m'_{ew}} + \eta \right)} \tag{17}$$

and  $I_\nu$  and  $K_\nu$  are the modified Bessel and Hankel functions, respectively, of order  $\nu$  for the variable  $\rho_1$ . (See Ref. 7.) The integrals of Bessel and Hankel functions appearing in Eq. (16) are tabulated in Ref. 8.

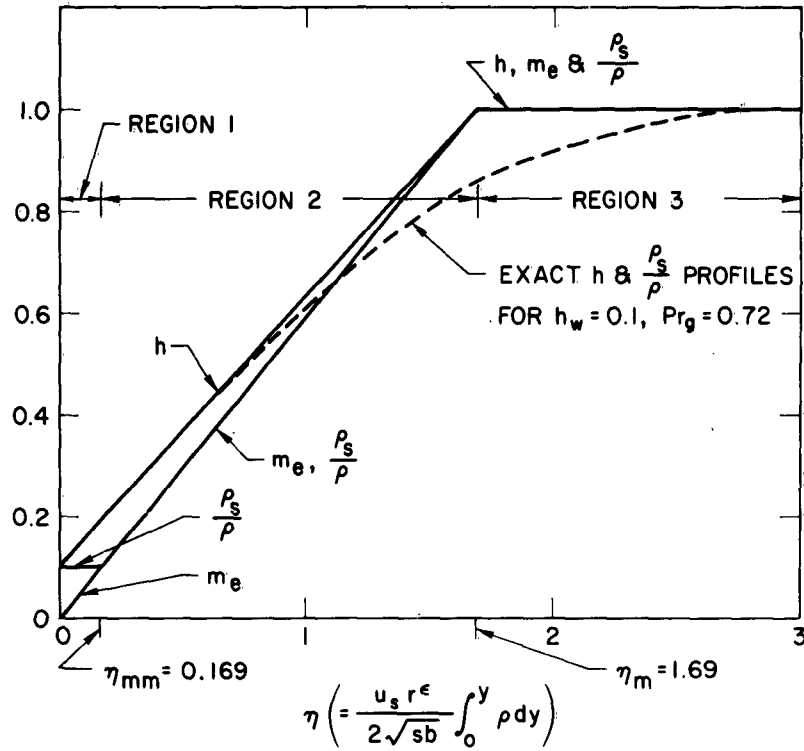


Figure 2. Approximate  $h$ ,  $m_e$  and  $\rho_s/\rho$  Profiles

For region 2 ( $\eta_{mm} \leq \eta \leq \eta_m$ )

$$\theta(\hat{\rho}_2) = \gamma_2 I_0 + \gamma_3 K_0 + \hat{\rho}_2 \left[ \left( h_w - \frac{h'_w}{m'_{ew}} m_{ew} \right) (K_1 I_0 + I_1 K_0) \right] + \left( \hat{\rho}_2^3 + 4\hat{\rho}_2 \right) \left[ \frac{h'_w m'_{ew}}{4Pr_e \Gamma_{el}} (K_1 I_0 + I_1 K_0) \right] \quad (18)$$

where

$$\hat{\rho}_2 = 2 \sqrt{\frac{\text{Pr}_e \Gamma_{el}}{m'_{ew}} \left( \frac{m_{ew}}{m'_{ew}} + \eta \right)} \quad (19)$$

and  $I_\nu$  and  $K_\nu$  are the modified Bessel and Hankel functions, respectively, of order  $\nu$  for the variable  $\hat{\rho}_2$ .

For region 3 ( $\eta_m \leq \eta$ )

$$\theta(\rho_3) = 1 + \gamma_4 H_N \int_{\rho_3}^{\infty} \frac{\exp(-\rho_3^2)}{H_N^2} d\rho_3 \quad (20)$$

where

$$\rho_3 = \sqrt{\text{Pr}_e} (\eta - 0.86038) \quad (21)$$

$$N = \frac{\Gamma_{el}}{2} \text{ (even integer)}$$

and  $H_N$  is the Hermite polynomial given by

$$\begin{aligned} H_N(\rho_3) = & (2\rho_3)^N - (N)(N-1)(2\rho_3)^{N-2} \\ & + \frac{(N)(N-1)(N-2)(N-3)}{2!} (2\rho_3)^{N-4} - \dots \end{aligned} \quad (22)$$

For extremely large values of  $N$ , appropriate asymptotic forms of the Hermite polynomials can be found in Ref. (9) and (10).

The four constants of integration,  $\gamma_1$  through  $\gamma_4$ , are determined by requiring that  $\theta$  and  $\theta'$  be continuous between regions 1 and 2, and 2 and 3, respectively.

The preceding solutions were obtained for the wall boundary condition  $\theta'_w = 0$ , which leads to an electron temperature jump at the wall. As mentioned previously, this wall boundary condition must be replaced by the "no-jump" condition of  $\theta_w = h_w$  for the special cases of  $m_{ew} > 10^{-2}$ . A solution of the electron energy equation satisfying the boundary condition  $\theta_w = h_w$  can be readily obtained in the same manner as the preceding ones. In the present study, however, we shall not analyze this special case except for  $\Gamma_{el} \rightarrow 0$ . The solution of Eq. (12) for  $\Gamma_{el} \rightarrow 0$  and a given  $\theta_w$  is:

For regions 1 and 2

$$\theta = \frac{(1 - \theta_w) \ln\left(1 + \frac{m'_{ew}}{m_{ew}} \eta\right)}{\ln(m_{ew}^{-1}) + \frac{\sqrt{\pi} m'_{ew} \exp(\rho_{3m}^2)}{2\sqrt{Pr_e}} (1 - \text{erf } \rho_{3m})} + \theta_w \quad (23)$$

For region 3

$$\theta = 1 - \frac{(1 - \theta_w)(1 - \text{erf } \rho_3)}{\frac{2\sqrt{Pr_e} \exp(-\rho_{3m}^2)}{\sqrt{\pi} m'_{ew}} \ln(m_{ew}^{-1}) + (1 - \text{erf } \rho_{3m})} \quad (24)$$

The linear profiles for  $h$  and  $m_e$  are chosen to give correct values of  $h_w$  and  $h'_w$ , and  $m_{ew}$  and  $m'_{ew}$ , respectively. The values of  $\eta_{mm}$  and  $\eta_m$ , therefore, are given by

$$\eta_{mm} = h_w \eta_m \quad (25)$$

and

$$\eta_m = \frac{1 - h_w}{h'_w}$$

when

$$Sc_a \approx Pr_g$$

Typical electron temperature profiles are given in Fig. 3 and will be discussed later.

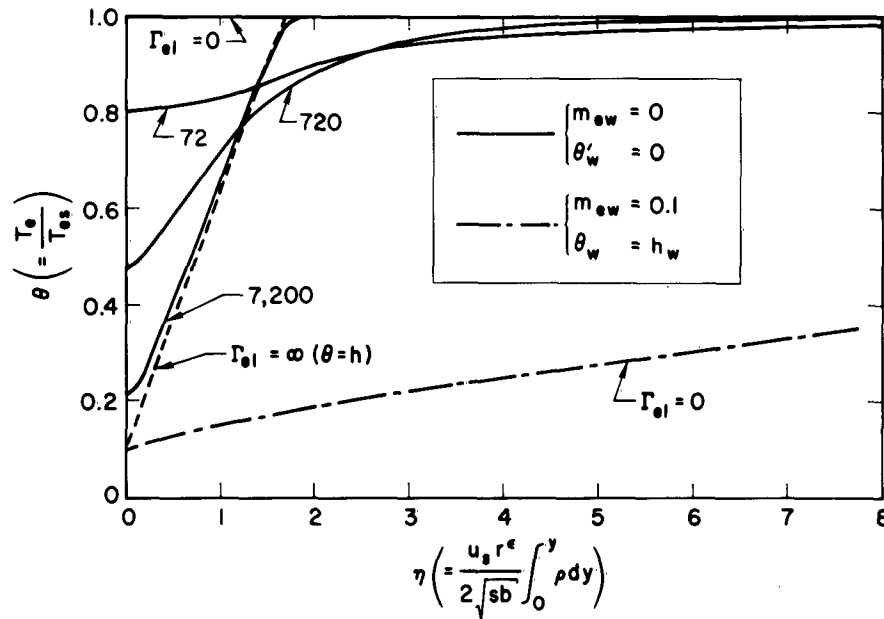


Figure 3. Nonequilibrium Electron Temperature Profiles for  $Pr_e = 10^{-3}$

In this section, we have analyzed the electron energy equation, Eq. (4), and obtained the electron temperature profiles for the various cases. In the following section, the conservation and the Poisson equations, Eqs. (1)-(3), will be analyzed by using the electron temperature distributions that have just been obtained.



#### IV. ELECTRICAL CHARACTERISTICS OF BOUNDARY LAYER

In the present section, the conservation and the Poisson equations, Eqs. (1), (2) and (3), will be solved. The boundary conditions to be satisfied are those explained earlier:  $m(\infty) = 1$ ,  $m(0) = 0$ , and the given  $(j_e/j_i)_w$ . The electrical characteristics of the boundary layer will then be studied.

The present study, like that in Ref. 2, is concerned with the regime in which the sheath thickness is much greater than the electron-neutral particle mean free path, but is much smaller than the thickness of the boundary layer. The method of solution is essentially the same as that given in Ref. 2 except that the more general cases of unequal ion and electron temperatures will be analyzed here where only the case of equal ion and electron temperatures was studied in Ref. 2.

The boundary layer is first divided into two arbitrary regions, the sheath and the ambipolar regions (see Fig. 1). Solutions will be obtained separately for the two regions and will then be matched at a suitable point.

In the remainder of this section an outline of the method of solution and results are given. Details of analysis will be found in Appendix B.

Within the thin sheath region presently of interest, the convection terms of Eqs. (1) and (2) can be neglected. Also, the temperature ratio  $T_i/T_e = (T_g/T_e)$  can be considered to be constant in the thin sheath without causing any undue error. The three coupled equations, Eqs. (1) through (3), with the above simplifications, are integrated by using a digital computer for various combinations of controlling parameters.

The ambipolar region is defined as that region of the boundary layer where the charge separation is negligible. Thus, in this region Poisson's

equation is extraneous. The conservation equations (1) and (2) then give the equation

$$\left(\frac{1}{Sc_a} m'\right)' + fm' = 0 \quad (26)$$

where

$$\frac{1}{Sc_a} = \frac{1}{Sc_i} \frac{\left(1 + \frac{T_e}{T_i}\right) \sqrt{\frac{M_i}{M_e}} \left(\frac{T_e}{T_i}\right)}{1 + \sqrt{\frac{M_i}{M_e}} \frac{T_e}{T_i}} \left\{ 1 + \frac{\left(1 + \frac{T_e}{T_i}\right)_0 \left[1 - \left(\frac{j_e}{j_i}\right)_w\right]}{\sqrt{\frac{M_i}{M_e}} \left(\frac{T_e}{T_i}\right) \left(1 + \frac{T_e}{T_i}\right) \left[1 + \sqrt{\frac{M_e}{M_i}} \left(\frac{T_i}{T_e}\right)_0 \left(\frac{j_e}{j_i}\right)_w\right]} \right\} \quad (27)$$

and the subscript 0 here represents the average value for the sheath region. For the regime presently of interest in which the ratios  $T_e/T_i$  and  $(j_e/j_i)_w$  are each no greater than  $\sim 10$ , Eq. (27) can be simplified to

$$\frac{1}{Sc_a} \approx \left(1 + \frac{T_e}{T_i}\right) \frac{1}{Sc_i} \quad (28)$$

For the case of equal electron and ion temperatures, the above equation gives the following familiar definition:

$$Sc_a \approx \frac{1}{2} Sc_i \quad (29)$$

Consistent with the approximations that we have made so far, we consider that  $Sc_a$  is constant across the ambipolar region. Such an approximation will not cause any undue error in the results because the solution of a diffusion equation such as Eq. (26) depends only weakly on the Schmidt number

( $\approx Sc_a^{1/3}$ ). Equation (26) then becomes the conventional boundary layer diffusion equation and the solution can be readily obtained in terms of the stream function  $f$  (see Ref. 11).

For the electric field intensity in terms of the  $m$  profile obtained above, the analysis of Eqs. (1) and (2) also yields the following equation:

$$E \cdot a \sqrt{\frac{\nu_s}{\beta l^2}} = \sqrt{\frac{1+\epsilon}{2}} \frac{1 - \sqrt{\frac{M_i}{M_e} \left(\frac{T_e}{T_i}\right)^2}}{1 + \sqrt{\frac{M_i}{M_e} \left(\frac{T_e}{T_i}\right)^2}} \times \frac{1}{m} \left\{ m' - \frac{\left[1 + \left(\frac{T_e}{T_i}\right)_0\right] \left[1 - \left(\frac{j_e}{j_i}\right)_w\right] m'_0}{\left[1 - \sqrt{\frac{M_i}{M_e} \left(\frac{T_e}{T_i}\right)^2}\right] \left[1 + \sqrt{\frac{M_e}{M_i} \left(\frac{T_i}{T_e}\right)_0} \left(\frac{j_e}{j_i}\right)_w\right]} \right\} \quad (30)$$

where  $(T_i/T_e)_0$  represents the average temperature ratio for the sheath region.

The complete solution of the original equations, Eqs. (1) through (3), for the boundary layer is now obtained by matching the numerical solution of the sheath region and the closed-form solution of the ambipolar region at  $\eta_0$  for  $m_i$ ,  $m_e$ ,  $m'_i$ ,  $m'_e$  and  $E$ , respectively.

The potential drop across the boundary layer is obtained by integrating the electric field intensity over the physical thickness of the boundary layer.

Figure 4 shows a typical solution of the sheath region obtained by the use of a digital computer. Figures 5a and 5b show typical  $m_e$ ,  $m_i$  and  $E$  profiles for the boundary layer. Figures 6 through 8 show the overall electrical characteristics of stagnation boundary layers, which will be discussed later.

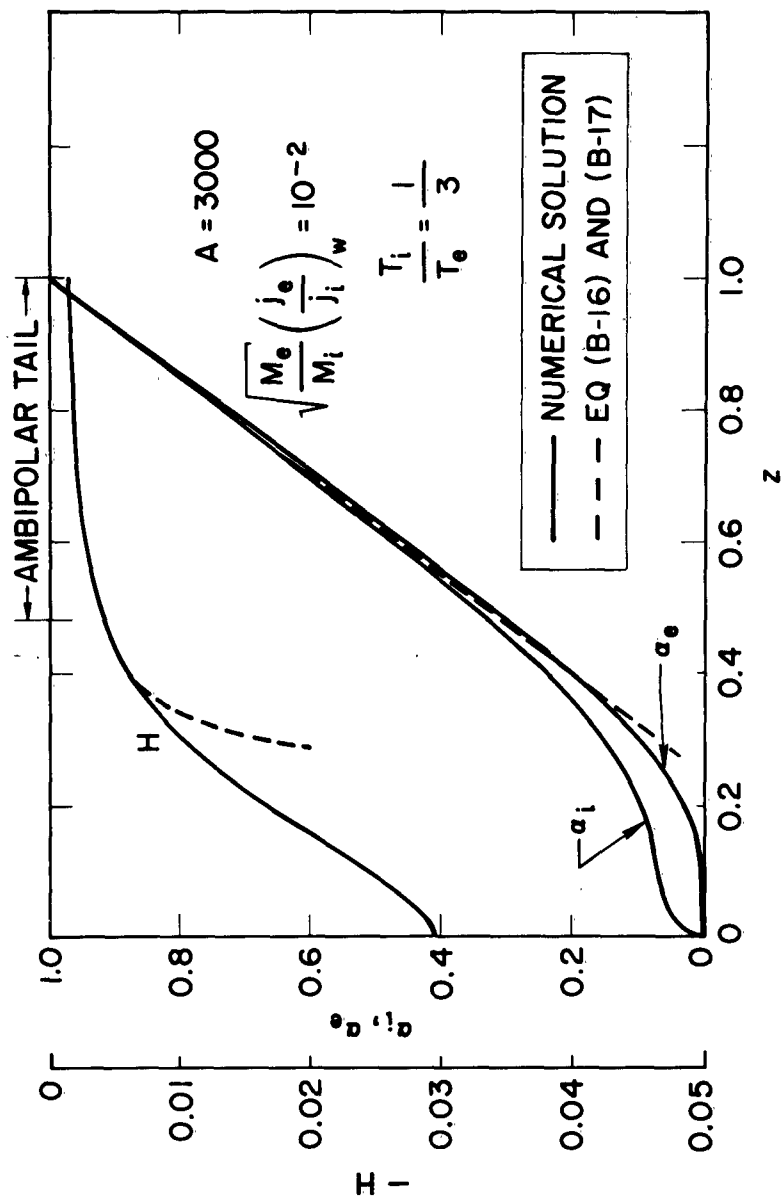


Figure 4. Typical Sheath Solution

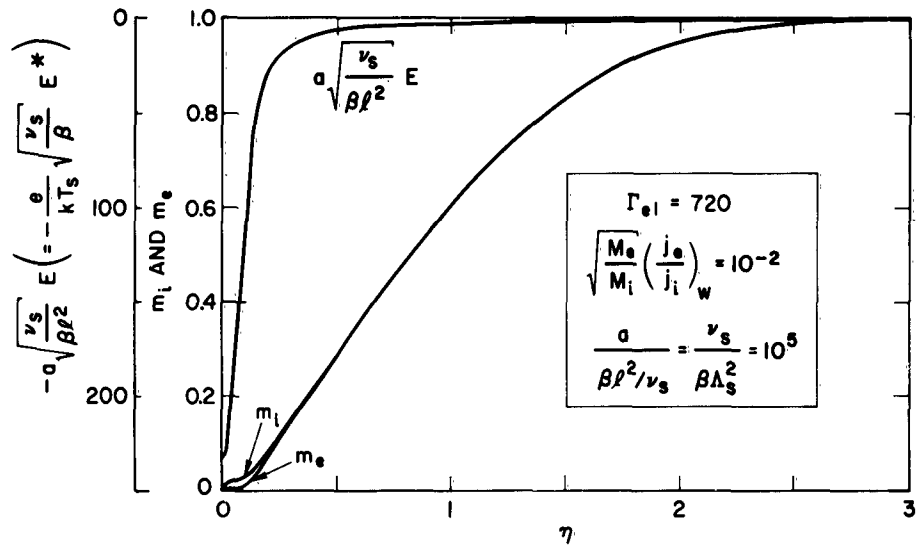


Figure 5a. Typical Electron, Ion, and Electric Field Distribution in Boundary Layer

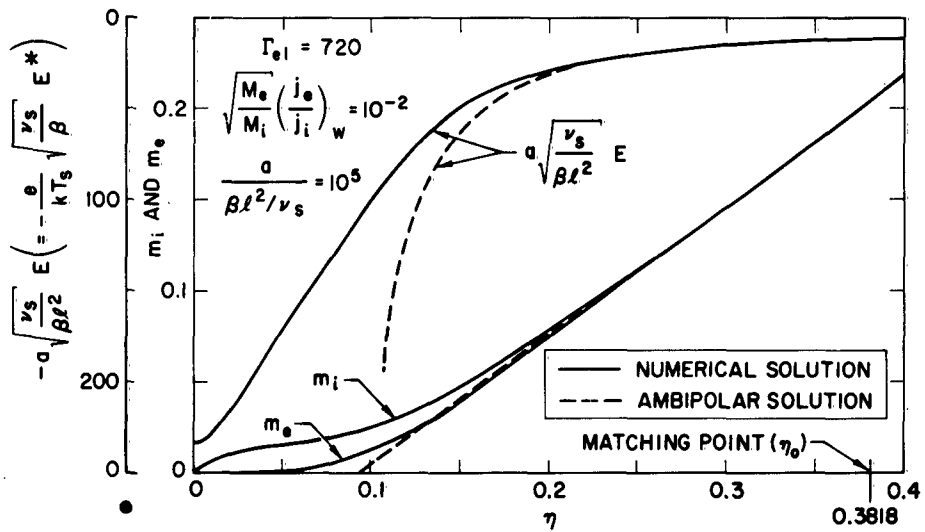


Figure 5b. Typical Electron, Ion, and Electric Field Distribution in Sheath Region

## V. DISCUSSION

Figure 3 shows the electron temperature profiles for the various values of the parameter  $\Gamma_{el}$  where  $\Gamma_{el}$ , defined by Eq. (14), represents the ratio of the characteristic convection time to the characteristic temperature equilibration time as explained previously. As  $\Gamma_{el}$  is increased from zero, the electron temperatures near the wall begin to decrease toward the neutral gas temperatures (Fig. 3). This initial relaxation, however, causes the electron temperatures in the outer portion of the boundary layer to deviate from the equilibrium temperatures (neutral gas temperatures). The reason for this is as follows. The rate of temperature equilibration for a given small value of  $\Gamma_{el}$  is much greater near the wall than in the outer portion of the boundary layer because the gas density and the differences between the electron and the neutral gas temperatures are much greater in the fluid near the wall than distant from it. The initial increase of  $\Gamma_{el}$ , therefore, causes mainly temperature relaxation near the wall. The decreased electron temperature near the wall then causes the temperature of the electrons in the outer portion to decrease by conducting the energy away from them.

This phenomenon thickens the electron thermal boundary layer substantially (Fig. 3). The rather large thickening is due to the extremely small magnitude of the electron Prandtl number that propagates the electron temperature disturbances near the wall through a considerable distance. Figure 3 shows that the electron energy boundary layer remains much thicker than the neutral gas thermal boundary layer until  $\Gamma_{el}$  becomes sufficiently large so that the temperature equilibration is nearly complete throughout the boundary layer. The complete temperature equilibration is seen to be accomplished at the value of  $\Gamma_{el}$  of  $\sim 10^4$ . According to Eq. (15), this means that for laboratory conditions of  $\beta T_s$  of the order of  $10^8$  °K/sec (commonly encountered), the complete temperature equilibration is not accomplished unless the stagnation point pressure is on the order of 100 atm. These criteria for the equilibrated

electron temperatures are seen to be much more severe than those commonly predicted previously (for instance, see Ref. 1). The reason for this is that the conventional criteria have usually been based on the comparison between the characteristic residence time for the electrons and the characteristic temperature equilibration time. The characteristic residence time of electrons is related to the electron current density given by the approximate expression of Eq. (A-6). The minimum residence time occurs when  $(j_e/j_i)_w$  is maximum ( $\sim 10$  in the present cases). Equation (A-6) shows that the residence time presently of interest is within about one order of magnitude of the ion diffusion time. As is mentioned following Eqs. (A-6) and (A-7), the parameter  $(Pr_e/Sc_i)$  represents the ratio of the characteristic conduction time of electron energy to the characteristic diffusion time of ions; this parameter is of the order of  $10^{-3}$ . Thus, the characteristic conduction time for electron energy is at least 100 times shorter than the characteristic electron residence time for the ranges of  $(j_e/j_i)_w$  considered in the present study. Therefore, it is the electron energy conduction time rather than the residence time that should be compared with the equilibration time in determining the nonequilibrium electron temperatures. From these arguments, therefore, it is seen that the parameter  $(Pr_e \Gamma_{el})$  that represents the ratio of the characteristic conduction time to the characteristic equilibration time is a more physically meaningful parameter for the prediction of temperature equilibration process than  $\Gamma_{el}$  alone. This can be also seen from the right-hand side of Eq. (12). Figure 3 shows that the temperature equilibration is nearly complete when  $Pr_e \Gamma_{el}$  is of the order of 10.

The semi-broken line in Fig. 3 shows the electron temperature for  $m_{ew} = 0.1$ ,  $\theta_w = h_w$ , and  $\Gamma_{el} \rightarrow 0$  obtained from Eqs. (23) and (24). As mentioned earlier, this is a special case of either a poorly catalytic surface or a highly seeded gas over a high temperature surface in which  $n_{ew}$  is within about one order of magnitude of  $n_{es}$ . These are highly special cases; however, the figure shows the drastic effect the wall could have on the electron temperatures of the boundary layer should such cases arise. Due to the extremely small

value of the electron Prandtl number, the cooling effect of the wall will be felt by most of the electrons in the shock layer.

It was mentioned earlier that the electron temperatures were expected to be rather insensitive to the detailed variation of the electron concentration profiles. This can be substantiated from the electron energy equation, Eq. (12), and the solutions of this equation. The electron concentration profile enters into Eq. (12) through the terms  $(m'_e/m_e)$  and  $(\rho/\rho_s)$ . The density ratio was made a function of  $m_e$  during the subsequent solution of the equation by letting  $\rho/\rho_s \approx m_e^{-1}$ . The effect of varying the electron concentration profile on the solution of the energy equation can be studied quite generally within the framework of the approximations given by Eqs. (A-14) through (A-17) by studying the effect of varying  $m'_{ew}$  on the electron temperatures. First, it can be seen from Eqs. (A-14) and (A-15) that

$$\frac{m'_e}{m_e} = \begin{cases} \frac{1}{\eta} & 0 \leq \eta \leq \eta_m \\ 0 & \eta > \eta_m \end{cases}, \quad \text{as } m'_{ew} \rightarrow 0$$

Thus,  $m'_e/m_e$  is essentially independent of  $m'_{ew}$  when  $m'_{ew} \rightarrow 0$ , which is the present case. Next, the effect of varying  $m'_{ew}$  on the right-hand side of Eq. (12), through its effect on  $\rho/\rho_s$ , is approximately of the same order as the effect of varying  $\Gamma_{el}$ . It is seen from the solutions of the equation given in Fig. 3 that a little variation of  $\Gamma_{el}$  (such as 10 to 20 percent) affects the electron temperatures very little. Thus, we have now shown that the electron temperatures are rather insensitive to the detailed variation of the electron concentration profiles. The above arguments can also be readily supported from the analytic solutions of Eq. (12), i. e., Eqs. (16), (18), and (20), by noting the very weak dependence of the solutions on  $m'_{ew}$ .

The preceding discussion leads to the following observation concerning the effect of the gas-phase electron-ion recombination on the electron



temperatures: According to Ref. 12, it seems that radiative two-body recombination is the predominant gas-phase recombination process when it occurs in gases such as argon. If this is true, then the effect of the recombination on the electron temperatures appears only through its effect on the electron concentration profile. It was shown in the preceding paragraph that the electron temperature is rather insensitive to the variation of electron concentration profile. Therefore, a moderate rate of radiative gas-phase recombination of ions and electrons will not appreciably affect the electron temperature profile. If the recombination, however, is predominantly a three-body process in which the electrons become the third body (catalyst), another energy source term must be added to the present electron energy equation and, therefore, the present solution is invalid.

Before leaving Fig. 3, we should mention that the electron temperature profile for the frozen limit of  $\Gamma_{el} = 0$  is not, strictly speaking, that of  $\theta = 1$  as given in the figure. In the analysis, the energy source term  $e j_e E^*$  appearing in the energy equation, Eq. (4), was neglected because it is of much smaller order of magnitude compared to the energy conduction term. This approximation, however, must fail in the limit of  $\Gamma_{el} = 0$  because in this limit the conduction term vanishes everywhere with the electron temperature gradient. The effect of the term  $e j_e E^*$  is to decrease the electron temperatures because  $E^*$  near the wall is negative, and the electron current density is toward the wall for all the cases considered in the present analysis. Therefore, the electron temperature profile in the limit of  $\Gamma_{el} \rightarrow 0$  will actually be much like that for a small value of  $\Gamma_{el}$  that gives a small but nonvanishing temperature gradient to balance the  $e j_e E^*$  term.

Figures 6, 7, and 8 show the typical variation of the potential difference and the current densities with respect to several major parameters.

The net potential difference across the boundary layer and the current density for the electron temperature profiles obtained in Fig. 3 and for  $(j_e/j_i)_w = 1$  assuming  $\sqrt{M_e/M_i} = 10^{-2}$  are shown in Fig. 6. The potential difference is

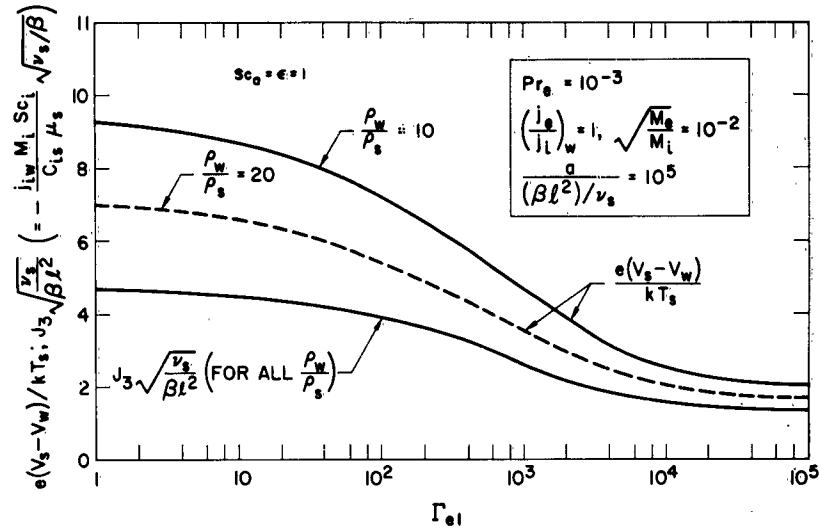


Figure 6. Floating Potential and Ion Current versus Equilibration Parameter

seen to increase as the temperature equilibration parameter  $\Gamma_{el}$  is decreased. This is to be expected, because the electron temperatures near the wall increased with decreasing  $\Gamma_{el}$  in Fig. 3; also, the sheath potential drop is seen (Ref. 2 and Table 1) to increase with the electron temperature. It is also seen in Fig. 6 that the ion current density increases in a manner similar to the potential difference as the electron temperature increases. It is interesting to note that a dependence of the ion current density on the electron temperature was also suggested for the free-fall sheath of a static plasma in the analysis of Ref. 13. Figure 6 shows that, for  $\rho_w/\rho_s$  between 10 and 20, the floating potential of the wall with respect to the plasma is increased by about 4 to 5 fold as  $\Gamma_{el}$  is varied from  $\infty$  to zero. The ion and electron current densities at the same time are seen to have increased by about four fold.

Figure 7 shows the variations of the floating potential and the ion current density with respect to the plasma flow parameter  $a(v_s/\beta l^2) = [v_s/\beta \Lambda_s^2]$  for

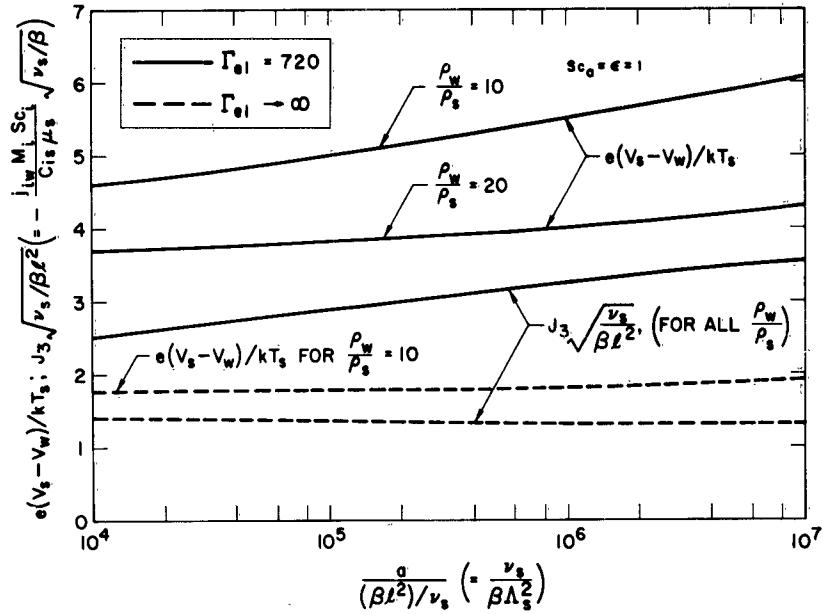


Figure 7. Floating Potential and Ion Current versus Plasma Flow Parameter

$\Gamma_{el} = 720$  and  $\Gamma_{el} = \infty$ , respectively. It is seen that the potential and the nondimensional ion current, as a whole, are rather insensitive to the variation of the flow parameter when the wall is highly cooled. These quantities, however, are seen to vary considerably more with the flow parameter for  $\Gamma_{el} = 720$ . The reason for this is that the sheath thickness varies with the flow parameter and thus the average temperature ratio  $T_i/T_e$  for the sheath is a function of the flow parameter. This dependence of the average temperature ratio on the sheath thickness, when the temperature equilibration is not complete, causes the potential difference and the nondimensional ion current density to be influenced to a greater extent by the parameter  $a \cdot (v_s / \beta l^2)$  than when  $T_i/T_e = 1$ . As is seen in Fig. 7 and Ref. 2, however, the potential difference varies with the density ratio  $\rho_w/\rho_s$  much more than with the flow

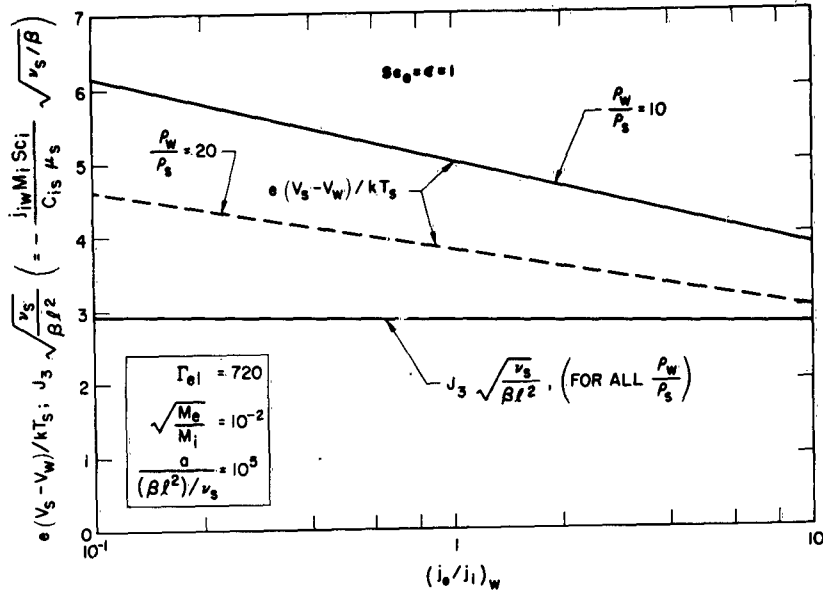


Figure 8. Potential Across Boundary Layer and Ion Current versus Current Ratio

parameter. The nondimensional ion current density  $J_3 \left[ v_s / (\beta l^2) \right]^{1/2}$  is independent of the density ratio  $\rho_w / \rho_s$ . The ion current density will be discussed subsequently in detail.

Figure 8 shows the typical variation of the potential difference across the boundary layer and the current density with respect to the ratio  $(j_e / j_i)_w$ . The figure, however, may be more conveniently interpreted as showing the effect on the ion and electron current densities of varying the potential difference. It is seen that as the potential difference<sup>2</sup> is increased from about 3.8 to 6.2 (for instance, at  $\rho_w / \rho_s = 10$ ) the nondimensional ion current density is increased only by about 10 percent. The electron current density, on the other

<sup>2</sup>Note that the wall potential is negative with respect to the plasma.

hand, is seen to have decreased by about two orders of magnitude, since  $j_{iw}$  remained essentially constant.

The following observations on the current densities can be made from Fig. 6, 7, and 8. The nondimensional ion current density  $J_3 \left[ v_s / (\beta l^{1/2}) \right]$  is a function of only the electron to ion temperature ratio and, thus, of the parameter  $\Gamma_{el}$ . The actual ion current density for a given electron temperature, therefore, is:

$$j_{iw} \sim \sqrt{\beta(\rho_s \mu_s)} \frac{C_{is}}{M_i Sc_i}$$

The parameter  $[\beta(\rho_s \mu_s)]^{1/2}$  is the parameter appearing in the usual boundary layer solutions for determining heat or mass transfer rate (see Refs. 14 and 15).  $C_{is}$  is the same as the degree of ionization in the plasma. For a given value of electron temperature and  $[\beta(\rho_s \mu_s)]^{1/2} [C_{is} / (M_i Sc_i)]$ , the variation of the potential drop does not vary the ion current appreciably within the present orders of magnitude. The electron current, however, is quite drastically affected by the potential drop.

Equation (30) shows that the electric field intensity vanishes identically at the edge of the diffusion boundary layer (where  $m' = 0$ ) only if  $(j_e / j_i)_w = 1$ . For all other cases, it shows that a nonvanishing field intensity exists at the boundary layer edge. This is consistent with the boundary layer characteristics and also with the physical problem itself. The supply of the charged particles to the boundary layer edge from the inviscid region is by convection and the drift due to the electric field. The convection supplies both the ions and the electrons at the same rate. Thus, an electric field is needed at the boundary layer edge to satisfy the condition of the unequal current densities when  $(j_e / j_i)_w \neq 1$ . Equation (30) shows that  $E_s$  is positive when  $(j_e / j_i)_w > 1$ , whereas it is negative when  $(j_e / j_i)_w < 1$ .

Strictly speaking, one can consider in a physical problem a solid surface in contact with a semi-infinite plasma only if the surface is electrically floating and, therefore,  $(j_e/j_i)_w = 1$ . The electric field intensity then must exactly disappear at infinity. The steady-state condition of  $(j_e/j_i)_w \neq 1$ , on the other hand, can be obtained only with the help of an external circuit. This means that there must be another electrode in contact with the plasma at a finite distance from the present surface. Therefore, the plasma is not, strictly speaking, semi-infinite and the electric field intensity beyond the boundary layer edge is not exactly zero, although it may be of much smaller order of magnitude than that within the boundary layer. Of course, there will be another boundary layer at the other electrode surface and an appropriate potential difference across it.

Let us consider the order of magnitude of the residual electric field intensity and its effect on the actual potential difference between the wall and the plasma. The magnitude of the electric field intensity at the boundary layer edge relative to that at the sheath edge can be readily obtained from Eq. (30). A simple estimate from Eq. (30) shows that the electric field intensity at the boundary layer edge is less than one percent of that at the sheath edge for  $(j_e/j_i)_w \leq 10$  and for the temperature ratios given in Fig. 3. For small probes located at a stagnation point, the three dimensional effect will quickly reduce such small electric field intensity to zero beyond the boundary layer edge; the potential drop beyond the boundary layer edge, compared to that across the boundary layer, may be neglected. The potential difference obtained for the boundary layer, therefore, is the potential difference between the wall and the plasma, for all practical purposes, when  $(j_e/j_i)_w \leq 10$ . When  $(j_e/j_i)_w \gg 10$ , however, Eq. (30) shows that the residual electric field intensity at the boundary layer edge can become the same order of magnitude as that at the sheath edge. For these cases, the electric field intensities that penetrate into the plasma in the inviscid region cannot be neglected and, therefore, the boundary layer treatment alone cannot describe the plasma-solid interaction satisfactorily.

## VI. RANGE IN WHICH THE THEORY IS VALID

In the present section, the regime of validity of the analysis based on the governing equations, Eqs. (1) through (4), will be examined.

### A. CONSERVATION AND POISSON EQUATIONS

There are three criteria that must be satisfied in order that the present solution of Eqs. (1) through (3) be valid:

1. Sheath thickness must be much greater than the mean free path.
2. The sheath must be sufficiently thin compared to the boundary layer so that the convection effect can be neglected within the sheath.
3. Gas-phase ion-electron recombination must be frozen.

The above criteria are the same as the first three criteria given in Ref. 2. The fourth criterion in Ref. 2 was  $T_e = T_i$ , but the present analysis removes this restriction. The first two criteria are rather straight-forward; the following expression derived in Ref. 2 for argon, for instance, specifies the criteria:

$$2 \times 10^6 \left( \frac{T_s \text{Re}}{l^2} \right) \leq n_s \ll 7 \times 10^{19} \left( \frac{p_s^2}{T_0} \right) \quad (31)$$

where

$$\text{Re} = \frac{u_\infty l}{\nu_s}$$

and  $T$  is in  $^\circ\text{K}$ ,  $l$  is in cm,  $n$  is in particles/cm<sup>3</sup>, and  $p$  is in atmospheres.

Nothing can be said with any certainty concerning criterion 3 because the gas-phase recombination process is not too well understood for the gases in the

present flow regimes. Assuming that the radiative gas-phase recombination sets in before the three body processes, the frozen recombination criterion may be expressed as

$$\frac{\tau_{\text{diff}}}{\tau_{\text{chem}}} \sim \frac{\delta \gamma n_s^2}{j_{iw}} \ll 1 \quad (32)$$

where the recombination coefficient  $\gamma$  for argon is about  $10^{-13}$  to  $10^{-10}$   $\text{cm}^3/\text{sec}$  (see Refs. 2 and 12), and  $\delta$  is the m-boundary layer thickness.

It is seen from the expressions (31) and (32) that a rather large regime of flow conditions can be analyzed by the present theory. It is shown in Ref. 2, for instance, that the three criteria are satisfied for the following typical conditions obtainable in an argon arc tunnel facility:

$$p_s = 0.1 \text{ atm}$$

$$l = 1 \text{ cm}$$

$$\text{Re} = 100$$

$$T_s = 7000^\circ\text{K}$$

$$T_0 = 500^\circ\text{K}$$

$$1.4 \times 10^{12} \leq n_{es} \ll 1.4 \times 10^{15}$$

It is also estimated in Ref. 2 (with some misgivings) that the above plasma condition may give equilibrated electron and neutral gas temperatures in the boundary layer. The estimate was based on the conventional comparison of



the temperature equilibration time with the characteristic electron residence time. According to the present analysis, however, the electron temperature will be far from being in equilibrium with the neutral gas temperature for the above flow conditions.

#### B. ELECTRON ENERGY EQUATION

There are two criteria which must be satisfied in order that the continuum electron energy equation, Eq. (4), be applicable for the weakly ionized gases presently of interest. The first is that the mean free path for the electrons between the electrons and the neutral gas particles be much smaller than the characteristic length of the flow. The mean free path between the electrons and the neutral gas particles is of the same order of magnitude as that between the neutral gas particles. This criterion is, therefore, essentially the basic one for the boundary layer flow itself; the conditions for the applicability of boundary layer theory have been well established elsewhere (for instance, see Ref. 16).

In addition to the above criterion for the basic boundary layer flow, the electrons must have a Maxwellian distribution such that the electron temperatures can be defined across the boundary layer in a continuous manner. Although the electron-neutral particle collisions aid the attainment of a Maxwellian distribution<sup>3</sup>, a conservative criterion for the distribution is based on the requirement that there be a sufficient number of electron-electron collisions during a suitable characteristic time for the electrons in the boundary layer. In order to verify the Maxwellian distributions of electrons between two electrodes, Kerrebrock compared (Ref. 18) the electron-electron collision time with the electron residence time. As was shown in the preceding section, however, the characteristic conduction time of electron thermal energy is much shorter than the characteristic electron

---

<sup>3</sup>It is shown in Ref. 17 that electron-neutral particle collisions alone in an electric field lead to an electron distribution which is usually between Maxwellian and Druyvesteyn distributions.

residence time when  $(j_e/j_1)_w \leq 10$ . The second criterion for the present problem is therefore satisfied when the electron-electron collision time is much shorter than the characteristic electron energy conduction time across the boundary layer. The characteristic electron-electron collision time  $\tau_{ee}$  is obtained from Spitzer (Ref. 19) as

$$\tau_{ee} = \frac{0.267 T_e^{3/2}}{n_e \ln \left[ \frac{3}{2e^3} \left( \frac{k^3 T_e^3}{\pi n_e} \right)^{1/2} \right]} \quad (33)$$

where  $\tau_{ee}$  is in sec,  $T_e$  is in  $^\circ\text{K}$ , and  $n_e$  is in particles/cm<sup>3</sup>. The logarithmic term of Eq. (33) is calculated and tabulated in Ref. 19. The conduction time of electron thermal energy  $\tau_c$  is given by

$$\tau_c \sim \left( \frac{\rho_e c_{pe}}{\lambda_e} \right) \frac{T_s \delta}{\left( \frac{\partial T_e}{\partial y} \right)} \sim \delta \text{Pr}_e \sqrt{\frac{2}{1+\epsilon}} \frac{1}{\beta \nu_s} \frac{\mu_s}{\mu} \frac{1}{\theta'} \quad (34)$$

Here  $\delta$  is the thickness of the electron thermal boundary layer.  $\theta'$  and  $\mu$  are some suitable average values for the boundary layer. The criterion is then satisfied when

$$\frac{\tau_{ee}}{\tau_c} \ll 1 \quad (35)$$

Although the normalized electron mass fraction  $m_e$  decreases monotonically from the boundary layer edge to the wall (Fig. 5), the number density  $n_e$  remains essentially constant almost all the way up to the wall because  $m_e \sim \rho_s / \rho$ . This has been noted in Ref. 20. Using  $n_e \approx n_{es}$  in Eq. (33), we can show that criterion (35) is satisfied for most of the flow conditions of interest to us, such as the example given in Sec. VI.A.

residence time when  $(j_e/j_i)_w \leq 10$ . The second criterion for the present problem is therefore satisfied when the electron-electron collision time is much shorter than the characteristic electron energy conduction time across the boundary layer. The characteristic electron-electron collision time  $\tau_{ee}$  is obtained from Spitzer (Ref. 19) as

$$\tau_{ee} = \frac{0.267 T_e^{3/2}}{n_e \ln \left[ \frac{3}{2e^3} \left( \frac{k^3 T_e^3}{\pi n_e} \right)^{1/2} \right]} \quad (33)$$

where  $\tau_{ee}$  is in sec,  $T_e$  is in  $^{\circ}\text{K}$ , and  $n_e$  is in particles/cm<sup>3</sup>. The logarithmic term of Eq. (33) is calculated and tabulated in Ref. 19. The conduction time of electron thermal energy  $\tau_c$  is given by

$$\tau_c \sim \left( \frac{\rho_e c_{pe}}{\lambda_e} \right) \frac{T_s \delta}{\left( \frac{\partial T_e}{\partial y} \right)} \sim \delta \text{Pr}_e \sqrt{\frac{2}{1+\epsilon}} \frac{1}{\beta v_s} \frac{\mu_s}{\mu} \frac{1}{\theta'} \quad (34)$$

Here  $\delta$  is the thickness of the electron thermal boundary layer.  $\theta'$  and  $\mu$  are some suitable average values for the boundary layer. The criterion is then satisfied when

$$\frac{\tau_{ee}}{\tau_c} \ll 1 \quad (35)$$

Although the normalized electron mass fraction  $m_e$  decreases monotonically from the boundary layer edge to the wall (Fig. 5), the number density  $n_e$  remains essentially constant almost all the way up to the wall because  $m_e \sim \rho_s/\rho$ . This has been noted in Ref. 20. Using  $n_e \approx n_{es}$  in Eq. (33), we can show that criterion (35) is satisfied for most of the flow conditions of interest to us, such as the example given in Sec. VI.A.

### C. WALL BOUNDARY CONDITIONS

Boundary conditions (9), (10) and (11) will now be derived.

Consider the interaction between the electrons at the interface  $w$  and the solid surface  $ww$ . The electron mass balance can be written as

$$\frac{1}{4} M_e \left[ (n\hat{v})_{ew} - (n\hat{v})_{eww} \right] = \left( \rho D_e \frac{\partial C_e}{\partial y} + \rho K_e E^* C_e \right)_w \quad (36)$$

When the surface is highly cooled and catalytic, the electron emission from the solid is negligible and, in addition, practically no electrons return to the interface after colliding with the surface. Therefore,  $n_{eww} \hat{v}_{eww} \rightarrow 0$  and Eq. (36), with the aid of Eq. (A-6), gives

$$m_{ew} \approx \left( \frac{5\pi}{8} \right) \sqrt{\left( \frac{T_g}{T_e} \right)_w} \frac{M_e}{M_g} \frac{1}{Sc_a} \left( \frac{j_e}{j_i} \right)_w \left( \frac{\hat{\lambda}_{gw}}{\delta} \right) \left( \frac{\partial m_e}{\partial y} \right)_0 \quad (37)$$

where  $\hat{\lambda}_g$  and  $\delta$  are the neutral gas mean free path and the boundary layer thickness, respectively. Equation (37) shows that

$$m_{ew} \sim 10^{-2} \left( \frac{j_e}{j_i} \right)_w \left( \frac{\hat{\lambda}_{gw}}{\delta} \right) \quad (38)$$

A similar analysis shows that

$$m_{iw} \sim \frac{\hat{\lambda}_{gw}}{\delta} \quad (39)$$

It is seen from Eqs. (38) and (39) that boundary conditions (9) and (10) are justified for all practical purposes when the surface is highly cooled and catalytic.

An electron energy balance can be written between the interface and the surface as

$$\frac{1}{4} M_e c_{pe} \left[ (n \hat{v} T)_{ew} - (n \hat{v} T)_{eww} \right] = \left[ \lambda_e \frac{\partial T_e}{\partial y} + c_{pe} T_e \left( \rho D_e \frac{\partial C_e}{\partial y} + \rho K_e E^* C_e \right) \right]_w$$

With the aid to Eqs. (36) and (A-3), the above equation becomes

$$\frac{1}{4} M_e (n \hat{v})_{eww} (T_{ew} - T_{eww}) = \frac{\mu_w}{Pr_e} \left( \frac{T_e}{T_g} \right)_w^{(1/2)+\sigma} C_{es} m_{ew} \left( \frac{\partial T_e}{\partial y} \right)_w \quad (40)$$

The above equation shows that  $(\partial T_e / \partial y)_w \rightarrow 0$  for highly cooled and catalytic surfaces since  $n_{eww} \hat{v}_{eww} \rightarrow 0$ . The boundary condition (11) is thus verified. Equation (40) shows that the electron temperature jump is maximum at the wall when the surface is highly cooled and catalytic, and thus no electrons reach the interface from the wall.

Let us now consider the other extreme, where no electron temperature jump exists at the wall. As mentioned previously, a no-jump condition exists, for instance, when either the surface is a poor catalyst, the surface temperature is much higher than about  $1000^\circ\text{K}$  and at the same time the surface has a very low work function, or when the gas adjacent to the high temperature surface is highly seeded. For such cases, the rate of electron transfer from the interface to the surface and that from the surface to the interface are of the same order of magnitude,  $n_{eww} \hat{v}_{eww} \sim n_{ew} \hat{v}_{ew}$ . The effect of the wall boundary condition on the electron temperature profile is maximum<sup>5</sup> when  $\Gamma_{el} \rightarrow 0$ . Thus, after substituting  $n_{ew} \hat{v}_{ew}$  for  $n_{eww} \hat{v}_{eww}$  and obtaining  $(\partial T_e / \partial y)_w$  from the frozen solution (23), Eq. (40) can be readily solved for the order of magnitude of  $n_{ew}$  that would make  $(T_{ew} - T_{eww}) \rightarrow 0$ . Such

<sup>5</sup>The electron temperature profile is almost independent of the wall boundary condition when  $\Gamma_{el} > 700$ .

analysis shows that, for many of the present flow regimes,  $m_{ew}$  must become the order of  $10^{-2}$  or so in order that the electron temperature jump can be neglected. This means that in order to neglect the temperature jump,  $n_{ew}$  must become approximately within one order of magnitude of  $n_{es}$ .

## VII. CONCLUDING REMARKS

An electron energy equation was formulated for weakly ionized stagnation boundary layers over highly cooled and catalytic surfaces. A solution was obtained analytically for electron temperature profiles that are not in equilibrium with the neutral gas temperatures. The effect of the nonequilibrium electron temperatures on the electrical characteristics of the boundary layer was then analyzed by solving the conservation equations of the charged particles and the Poisson equation.

It is found that, when the electron temperature is in equilibrium with the neutral gas temperature in the inviscid region, the potential difference across the boundary layer and the current densities increase about four to five times as the electron temperatures in the boundary layer vary from the completely equilibrium state to completely frozen state with respect to the neutral gas temperatures.

Though the variation of the electron temperatures affected the ion current and the potential difference alike, a variation of the potential difference alone for a given electron temperature was found to have a negligible effect on the ion current. On the other hand, the electron current was found to be drastically affected by the variation of the potential difference.

The state of the electron temperatures with respect to the neutral gas temperatures in the boundary layer was found to be controlled by the parameter  $(Pr_e \Gamma_{el})$  which represents the ratio of the characteristic electron energy conduction time to the characteristic temperature equilibration time. This parameter in the regime presently of interest,  $[10^{-1} \leq (j_e/j_i)_w \leq 10]$ , was found to be about two to three orders of magnitude smaller than the ratio of the characteristic electron residence time to the temperature equilibration time. The latter ratio has been conventionally used to determine the state of the electron temperatures. The present analysis shows, therefore, that the

electron-neutral gas temperature equilibration is accomplished at much higher pressures, for instance, than those previously expected.

The special cases of poorly catalytic surfaces and the highly seeded gas adjacent to high temperature surfaces were considered. It was shown that the cooling effect of the wall can have a drastic effect on the electron temperatures of the boundary layer should these conditions cause the electron concentration at the wall to become within one order of magnitude of that at the inviscid region.



Table I. Electrical Sheath Characteristics

$T_i/T_e$	A	$\sqrt{M_e/M_i} \left( \frac{j_e}{j_i} \right)_w$	$J_1$	$-\int_0^1 \text{Hdz}$	$-\int_0^1 z \text{Hdz}$
1	3000	$10^{-3}$ $10^{-2}$ $10^{-1}$	2.38 2.34 1.94	$0.33 \times 10^{-2}$ $0.24 \times 10^{-2}$ $0.144 \times 10^{-2}$	$0.6 \times 10^{-3}$ $0.42 \times 10^{-3}$ $0.31 \times 10^{-3}$
1/2		$10^{-3}$ $10^{-2}$ $10^{-1}$	4.01 3.69 3.22	$0.703 \times 10^{-2}$ $0.539 \times 10^{-2}$ $0.362 \times 10^{-2}$	$0.154 \times 10^{-2}$ $0.119 \times 10^{-2}$ $0.835 \times 10^{-3}$
1/3		$10^{-3}$ $10^{-2}$ $10^{-1}$	5.82 5.30 4.62	$0.108 \times 10^{-1}$ $0.845 \times 10^{-2}$ $0.589 \times 10^{-2}$	$0.25 \times 10^{-2}$ $0.201 \times 10^{-2}$ $0.143 \times 10^{-2}$
1/4		$10^{-3}$ $10^{-2}$ $10^{-1}$	7.79 7.02 6.1 •	$0.148 \times 10^{-1}$ $0.116 \times 10^{-1}$ $0.822 \times 10^{-2}$	$0.376 \times 10^{-2}$ $0.291 \times 10^{-2}$ $0.208 \times 10^{-2}$
1/6		$10^{-3}$ $10^{-2}$ $10^{-1}$	12.17 10.79 9.28	$0.227 \times 10^{-1}$ $0.179 \times 10^{-1}$ $0.130 \times 10^{-1}$	$0.627 \times 10^{-2}$ $0.485 \times 10^{-2}$ $0.351 \times 10^{-2}$

## NOMENCLATURE

A	parameter defined by Eq. (B-4)
a	parameter defined by Eq. (B-9)
b	constant defined by Eq. (A-10)
C	mass fraction
$c_{pe}$	specific heat of electrons per unit mass of electrons
D	binary diffusion coefficient
E	nondimensional electric field intensity defined by Eq. (B-9)
E*	electric field intensity
e	absolute charge of an electron
f	Blasius stream function
$G_1, G_2, G_3$	parameter defined by Eq. (B-20)
H	nondimensional electric field intensity defined by Eq. (B-4)
$H_N$	Hermite polynomial of order N
h	$T_g/T_s$
$I_\nu$	modified Bessel function of order $\nu$
$J_1$	nondimensional ion current density defined by Eq. (B-4)
$J_3$	nondimensional ion current density defined by Eq. (B-12)
j	particle current density
K	mobility
$K_\nu$	modified Hankel function of order $\nu$
k	Boltzmann constant
L	physical thickness of sheath region

$l$	nose radius
$M$	particle mass
$m$	$C/C_s$
$N$	even integer defined by Eq. (21)
$n$	charged particle number density
$p$	pressure
$Pr_e$	electron Prandtl number defined by Eq. (13)
$Pr_g$	Prandtl number of neutral gas
$Q_c$	Coulomb collision cross section
$Q_{eg}$	collision cross section between electrons and neutral particles
$Re$	Reynold's number
$r$	distance shown in Fig. 1
$s$	variable defined by Eq. (A-9)
$Sc_a$	ambipolar Schmidt number defined by Eq. (27)
$Sc_e$	electron Schmidt number
$Sc_i$	ion Schmidt number
$T$	temperature
$u$	x-component of velocity
$V$	potential
$v$	y-component of velocity
$\hat{v}_e$	electron mean thermal speed
$W_{el}$	energy transfer to electrons per unit time per unit volume due to elastic collision
$x$	streamwise distance

$y$	distance normal to surface
$z$	variable defined by Eq. (B-4)
$\alpha$	$C/C_0$
$\beta$	$du_s/dx$
$\Gamma_{el}$	temperature equilibration parameter defined by Eq. (14)
$\gamma_1, \gamma_2, \dots$	constants of integration
$\gamma_{eg}$	constant portion of $Q_{eg}$ defined by Eq. (A-5)
$\Delta$	modified thickness of sheath region defined by Eq. (B-4)
$\epsilon$	$\begin{cases} 0 & \text{for two dimensional body} \\ 1 & \text{for axisymmetric body} \end{cases}$
$\eta$	variable defined by Eq. (A-10)
$\theta$	$T_e/T_s$
$\Lambda$	Debye shielding length, $\sqrt{(kT_g)/(e^2 n_e)}$
$\lambda_e$	thermal conductivity of electrons
$\mu, \nu$	viscosity and kinematic viscosity, respectively.
$\rho$	density
$\rho_1, \rho_2, \rho_2', \rho_3$	variables defined by Eqs. (17), (A-23), (19) and (21), respectively
$\tau$	characteristic time

#### SUBSCRIPTS

$e$	electrons
$g$	neutral gas
$i$	ions
$m$	matching point between regions 2 and 3
$mm$	matching point between regions 1 and 2

s	edge of boundary layer
w	wall
ww	solid surface
v	integer
0	matching point between sheath and ambipolar regions unless specified otherwise

NOTE: Symbols without the subscript "e" or "i" refer to neutral gas.

## APPENDIX A

### Supplement to Analysis of Electron Energy Equation

The details leading to the solution of the electron energy equation are given in the following paragraphs.

#### I. Fundamental Property Values for the Electron Energy Equation

The electron thermal conductivity  $\lambda_e$  and the energy source terms  $W_{e1}$  and  $e j_e E^*$  will be studied in this section.

Consider first the electron thermal conductivity  $\lambda_e$ . Fay (Ref. 3) gives

$$\lambda_e = \frac{75\pi}{128} \frac{k n_e \bar{v}_e}{(n_g Q_{eg} + \sqrt{2} n_e Q_c)} \quad (\text{A-1})$$

The Coulomb cross section  $Q_c$  is about two orders of magnitude greater than the electron-neutral cross section  $Q_{eg}$  so that the second term in the denominator dominates for highly ionized plasma ( $n_e/n_g \gg 10^{-2}$ ) and  $\lambda_e$  is independent of  $n_e$ . In the weakly ionized plasmas ( $n_e/n_g \ll 10^{-2}$ ) of current interest, the first term predominates and  $\lambda_e$  is practically a linear function of  $n_e$ . It can be seen from data in Ref. 6 and other available data that

$$\frac{Q_{eg}}{Q_{gg}} \approx \frac{1}{2} \left( \frac{T_g}{T_e} \right)^\sigma \quad (\text{A-2})$$

where  $-1/2 \lesssim \sigma \lesssim 1/2$ , depending on the gas and temperature range. Equation (A-1) can be written as

$$\lambda_e = (\mu_{pe}) \left( \frac{T_e}{T_g} \right)^{(1/2)+\sigma} \frac{C_e}{Pr_e} \quad (A-3)$$

where

$$Pr_e = \frac{Pr_g \left( \frac{M_e}{M_g} \right)^{1/2}}{2^{3/2}} \quad (13)$$

We shall call  $Pr_e$ , defined by Eq. (13), the electron Prandtl number. As will be seen subsequently,  $Pr_e$  influences the behavior of the electron thermal boundary layer in a manner similar to the usual influence of the Prandtl number on the conventional thermal boundary layer. The electron Prandtl number is of the order of  $10^{-3}$  for most gases.

As in Ref. 2, the present study is limited to the regime  $10^{-1} \lesssim (j_e/j_i)_w \lesssim 10$ . Certain simplifications of the electron energy equation are possible in this regime. The electron energy source term  $e j_e E^*$  represents the rate at which electrons gain and lose energy due to their motion in the electric field. Using values of  $j_e$  and  $E^*$  obtained from Eq. (4) and Ref. 2, it can be shown that this term is negligible compared to the conduction terms in the ambipolar region. The electron temperatures, therefore, are practically unaffected by the electric field in most of the boundary layer. In the sheath, however, this term can become of the order of, or even greater than, the conduction term, depending on the magnitude of  $E^*$ . However, for  $10^{-1} \leq (j_e/j_i)_w \leq 10$ , it can be seen from Ref. 2 that  $E^*$  will be small enough so that this term, when compared to the conduction term, can be neglected even in the sheath. The main reason for this is that the conduction of energy takes place very efficiently because of the high mobility of the electrons. This fact can also

be seen from the extremely small value of  $Pr_e$  as given by Eq. (13). In this analysis, therefore, the term  $e j_e E^*$  is neglected.

Finally, the energy source term  $W_{el}$  is considered. This term represents the rate of energy exchange between electrons and the rest of the gas due to elastic collisions. Petchek and Byron have given (Ref. 4) a basic expression for  $W_{el}$  although the final expression they derived is not applicable to the present problem because they were interested in plasmas in which the Coulomb interaction predominates, i. e., in which most of the energy exchange is between electrons and ions. For the weakly ionized gases of current interest, most of the energy exchange is between electrons and neutrals. The basic equation in Ref. 4, however, may be used to derive the following equation, which is valid for weakly ionized plasmas (much less than one percent):

$$W_{el} = 3\sqrt{3} \gamma_{eg} \sqrt{\frac{k^3}{M_e}} \left( \frac{M_e}{M_g} \right) n_e n_g (T_g - T_e) \quad (A-4)$$

Here it has been considered that the collision cross section between electrons and neutrals has the form:

$$Q_{eg} = \frac{\gamma_{eg}}{\sqrt{T_e}} \quad (A-5)$$

The above expression can be derived from information in Ref. 6 for high temperature air.



## II. Simplification and Transformation of the Electron Energy Equation

The equation has already been simplified by decoupling it from the conservation and Poisson equations (see text) and by neglecting the term  $e j_e E^*$ . One additional basic simplification will be made before attempting the solution.

It can be readily shown from Eqs. (1) and (2) that for the predominantly ambipolar boundary layer considered here:

$$\rho D_e \frac{\partial C_e}{\partial y} + \rho K_e E^* C_e \approx \left( \frac{j_e}{j_i} \right)_w \left( 1 + \frac{T_e}{T_i} \right) \rho D_i \frac{\partial C_e}{\partial y} \quad (\text{A-6})$$

This approximate equality is sufficient for the immediate purpose of showing that the term  $[\rho D_e (\partial C_e / \partial y) + \rho K_e E^* C_e]$  can be neglected in the electron energy equation. With the aid of Eqs. (5), (A-3), (13) and (A-6) the energy equation may be written:

$$\begin{aligned} \rho u \frac{\partial T_e}{\partial x} + \rho v \frac{\partial T_e}{\partial y} = \frac{1}{Pr_e} \frac{\partial}{\partial y} \left[ \left( \frac{T_e}{T_g} \right)^{(1/2)+\sigma} \mu \frac{\partial T_e}{\partial y} \right] + \frac{W_{el}}{C_e c_{pe}} \\ + \frac{\mu}{C_e Pr_e} \left( \frac{T_e}{T_g} \right)^{(1/2)+\sigma} \left( \frac{\partial T_e}{\partial y} \right) \left( \frac{\partial C_e}{\partial y} \right) \left[ 1 + \left( \frac{j_e}{j_i} \right)_w \frac{\left( 1 + \frac{T_e}{T_i} \right) Pr_e}{\left( \frac{T_e}{T_g} \right)^{(1/2)+\sigma} Sc_i} \right] \end{aligned} \quad (\text{A-7})$$

The present analysis is concerned with cases in which  $T_e$  and  $T_i$ , and  $j_e$  and  $j_i$ , differ by no more than an order of magnitude or so (see text). For these cases the term  $[(j_e/j_i)_w (1 + T_e/T_i) (Pr_e) / (T_e/T_g)^{(1/2)+\sigma} (Sc_i)] \ll 1$  and may be neglected. This is because the ratio  $Pr_e/Sc_i$ , which may be interpreted as an electron Lewis number, is much smaller than unity and, therefore, the

electron energy transfer (of the energy  $c_{pe} T_e$  only) due to concentration gradient and electric field motivated diffusion is negligible compared to the energy transfer due to thermal conduction. Such is not the case, for instance, if the wall is strongly and positively biased with respect to the plasma; then,  $(j_e/j_i)_w \gg 10$ . The electron energy equation, Eq. (4), now takes the form:

$$\rho u \frac{\partial T_e}{\partial x} + \rho v \frac{\partial T_e}{\partial y} = \frac{1}{Pr_e C_e} \frac{\partial}{\partial y} \left[ \mu \left( \frac{T_e}{T_g} \right)^{(1/2)+\sigma} C_e \frac{\partial T_e}{\partial y} \right] + \frac{W_{el}}{C_e c_{pe}} \quad (A-8)$$

To solve the above equation, we will first transform the equation to a similarity form at the stagnation region. Let

$$s = \int_0^x \rho_s \mu_s u_s r^{2\epsilon} dx = \frac{\rho_s \mu_s}{2(1+\epsilon)} \beta x^{2(1+\epsilon)} \quad (A-9)$$

and

$$\eta = \frac{u_s r^\epsilon}{2\sqrt{s}b} \int_0^y \rho dy \quad (A-10)$$

where

$$b = \frac{\rho \mu}{\rho_s \mu_s} = \text{constant}$$

Also, we define the following nondimensional quantities:

$$\theta = T_e/T_s, \quad h = T_g/T_s, \quad m_e = C_e/C_s \quad (A-11)$$

With the aid of Eq. (A-4) and Eqs. (A-9) through (A-11), Eq. (A-8) then becomes

$$\frac{1}{\text{Pr}_e} \frac{1}{m_e} \frac{d}{d\eta} \left[ \left( \frac{\theta}{h} \right)^{1/2+\sigma} m_e \frac{d\theta}{d\eta} \right] + f \frac{d\theta}{d\eta} = -\Gamma_{el} \left( \frac{\rho}{\rho_s} \right) (h - \theta) \quad (\text{A-12})$$

where  $\Gamma_{el}$  is given by Eq. (14). The stream function  $f$ , appearing in Eq. (A-12), is the solution of the Blasius momentum equation:

$$f''' + ff'' = 0 \quad (\text{A-13})$$

having the boundary conditions  $f(0) = f'(0) = 0$  and  $f'(\infty) = 2$ . The solution of Eq. (A-13) is found in Ref. 5.

### III. Solution of Electron Energy Equation

To solve the equation analytically, we make the following simplifications. First, the quantity  $m_e (\theta/h)^{1/2+\sigma}$  represents essentially the variation of  $\lambda_e$ . For the values of  $-1/2 \leq \sigma \leq 1/2$ ,  $(\theta/h)^{1/2+\sigma}$  varies very slowly compared to  $m_e$ , which varies from zero to 1 across the boundary layer. It is assumed, therefore, that  $(\theta/h)^{1/2+\sigma} = 1$  when compared to the variation of  $m_e$ . With this assumption, Eq. (A-12) is linearized as

$$\theta'' + \left( \frac{m'_e}{m_e} + \text{Pr}_e f \right) \theta' = -\text{Pr}_e \Gamma_{el} \left( \frac{\rho}{\rho_s} \right) (h - \theta) \quad (12)$$

Next, consider the parenthesized quantity in the second term of Eq. (12). It is seen that  $\text{Pr}_e f \ll m'_e/m_e$  for most portions of the boundary layer. Only in the outer portion of the boundary layer does  $\text{Pr}_e f$  become of the same order as  $m'_e/m_e$ , and, in the limit of  $y \rightarrow \infty$ ,  $\text{Pr}_e f$  becomes greater than

$m'_e/m_e$  as  $m'_e \rightarrow 0$ . Also, it was stated earlier that the electron temperature profile will be rather insensitive to the details of variation of  $m_e$  profile. With the above facts in mind, we subdivide the electron thermal boundary layer into three regions (Fig. 2) and the following simplifying approximations are made for the respective regions:

For regions 1 and 2 ( $0 \leq \eta \leq \eta_m$ )

$$\text{Pr}_e f = 0$$

$$h = h_w + h'_w \eta \quad (\text{A-14})$$

$$m_e = m_{ew} + m'_{ew} \eta$$

For region 3 ( $\eta \geq \eta_m$ )

$$f = 2(\eta - 0.86038) \quad (\text{A-15})$$

$$h = m_e = 1$$

For region 1 ( $0 \leq \eta \leq \eta_{mm}$ )

$$\rho = \rho_w \quad (\text{A-16})$$

For region 2 ( $\eta_{mm} \leq \eta \leq \eta_m$ )

$$\rho_s/\rho = m_e \quad (\text{A-17})$$

$\eta_m$  and  $\eta_{mm}$  are given by Eq. (25). The above approximations are comprised of replacing the  $h$  and  $m_e$  profiles by a pair of linear profiles and of letting  $\rho_s/\rho$  essentially follow  $m_e$  instead of  $h$ . A replacement of

boundary layer profiles by linear profiles is quite conventional practice, and the  $m_e$  and  $h$  profiles differ very little. The approximations, therefore, given by Eqs. (A-14) through (A-17) should create no great error in the results. The quantities  $h'_w$  and  $m'_{ew}$  will be obtained from the exact solution of the neutral gas energy equation and the exact ambipolar solution of the conservation equations, respectively. The expression for the stream function  $f$  given in Eq. (A-15) is obtained from Ref. 11 for the outer region of the boundary layer. As was explained earlier,  $m_{ew} = 0$  for all practical purposes when the surface is highly cooled and catalytic. However,  $m_{ew}$  will be retained in the analysis for the purpose of generality.

It is readily seen from Eq. (12) that in the outer portion of the boundary layer, where  $m'_e/m_e \ll Pr_e f$ , Eq. (12) becomes identical in form to the conventional thermal boundary layer equations with a Prandtl number equal to  $Pr_e$ . Thus,  $Pr_e$  influences the electron energy boundary layer in a manner similar to the influence of the regular Prandtl number on the conventional thermal boundary layer.

In the following, the electron energy equation, Eq. (12), will be solved subject to the simplifications mentioned above for each region; the solutions will then be matched at  $\eta_{mm}$  and  $\eta_m$  for  $\theta$  and  $\theta'$ , respectively. The boundary conditions for Eq. (12) are

$$\theta'(0) = 0 \quad (A-18)$$

$$\theta(\infty) = 1 \quad (A-19)$$

For region 1, Eq. (12) becomes:

$$\theta'' + \frac{1}{\left(\frac{m_{ew}}{m'_e} + \eta\right)} \theta' - \frac{Pr_e \Gamma_{el}}{h_w} \theta = -\frac{Pr_e \Gamma_{el}}{h_w} (h_w + h'_w \eta) \quad (A-20)$$

Let

$$\rho_1 = \sqrt{\frac{\text{Pr}_e \Gamma_{el}}{h_w} \left( \frac{m_{ew}}{m'_{ew}} + \eta \right)} \quad (\text{A-17})$$

Equation (A-20) is then transformed to the following inhomogeneous modified Bessel equation of zeroth order:

$$\frac{d^2 \theta}{d\rho_1^2} + \frac{1}{\rho_1} \frac{d\theta}{d\rho_1} - \theta = - \left[ \left( h_w - h'_w \frac{m_{ew}}{m'_{ew}} \right) + h'_w \sqrt{\frac{h_w}{\text{Pr}_e \Gamma_{el}}} \rho_1 \right] \quad (\text{A-21})$$

The solution of the above equation that satisfies the boundary condition (A-18) is obtained as Eq. (16).

For region 2, Eq. (12) becomes:

$$\theta'' + \frac{1}{\left( \frac{m_{ew}}{m'_{ew}} + \eta \right)} \theta' - \frac{\text{Pr}_e \Gamma_{el}}{m'_{ew}} \frac{1}{\left( \frac{m_{ew}}{m'_{ew}} + \eta \right)} \theta = -\text{Pr}_e \Gamma_{el} \left( \frac{h'_w}{m'_{ew}} \right) \left( \frac{\frac{h_w}{h'_w} + \eta}{\frac{m_{ew}}{m'_{ew}} + \eta} \right) \quad (\text{A-22})$$

Let

$$\rho_2 = \frac{\text{Pr}_e \Gamma_{el}}{m'_{ew}} \left( \frac{m_{ew}}{m'_{ew}} + \eta \right) \quad (\text{A-23})$$

Equation (A-23) is then transformed into

$$\frac{d^2 \theta}{d\rho_2^2} + \frac{1}{\rho_2} \frac{d\theta}{d\rho_2} - \frac{1}{\rho_2} \theta = - \left[ \left( h_w - h'_w \frac{m_{ew}}{m'_{ew}} \right) \frac{1}{\rho_2} + \frac{h'_w m'_{ew}}{\text{Pr}_e \Gamma_{el}} \right] \quad (\text{A-24})$$

The above is another modified form of an inhomogeneous Bessel equation and the solution is given by Eq. (18).

For region 3, Eq. (12) becomes the following homogeneous Hermite equation:

$$\frac{d^2 \hat{\theta}}{d\rho_3^2} + 2\rho_3 \frac{d\hat{\theta}}{d\rho_3} - \Gamma_{el} \hat{\theta} = 0 \quad (\text{A-25})$$

where

$$\rho_3 = \sqrt{\text{Pr}_e} (\eta - 0.86038) \quad (\text{21})$$

$$\hat{\theta} = 1 - \theta \quad (\text{A-26})$$

If we let

$$\Gamma_{el} = 2N$$

where  $N$  is an even integer, a particular solution of Eq. (A-25) is the Hermite polynomial given by Eq. (22). The general solution of Eq. (A-25) that satisfies boundary condition (A-19) is obtained as Eq. (20).

The constants of integration  $\gamma_1$  through  $\gamma_4$  are determined by requiring that  $\theta$  and  $\theta'$  be continuous between regions 1 and 2, and 2 and 3, respectively.

## APPENDIX B

### Supplement to Electrical Characteristics of Boundary Layer

Details of the solutions of Eqs. (1), (2), and (3) will be given in the following paragraphs. As explained in the text, the solutions will be obtained for the sheath and the ambipolar regions (Fig. 1), and the two solutions will be matched at a suitable point. The electron temperature distribution is assumed to be known (Appendix A).

#### I. Sheath Region

The convection terms of Eqs. (1) and (2) can be neglected in the thin sheaths presently of interest. Equations (1) through (3) then become the equations as derived in Ref. 2.

$$\frac{da_i}{dz} - AHa_i = J_1 \quad (\text{B-1})$$

$$\frac{da_e}{dz} + \frac{T_i}{T_e} AHa_e = J_1 \left( \frac{Sc_e}{Sc_i} \right) \left( \frac{j_e}{j_i} \right)_w = J_1 \sqrt{\frac{M_e}{M_i}} \left( \frac{T_i}{T_e} \right)^2 \left( \frac{j_e}{j_i} \right)_w \quad (\text{B-2})$$

$$\frac{dH}{dz} = a_i - a_e \quad (\text{B-3})$$



where

$$a = C/C_0 \quad (\text{B-4})$$

$$J_1 = -\frac{j_{iw} M_i S c_i \Delta}{C_{i0} \mu_0}$$

$$A = \frac{\Delta^2}{(kT_0/e^2 n_0)} = \left(\frac{\Delta}{\Lambda_0}\right)^2$$

$$z = \frac{\int_0^y \rho/\rho_0 dy}{\Delta}$$

$$\Delta = \int_0^L \rho/\rho_0 dy$$

$$H = \frac{E^*}{en_0 \Delta}$$

The boundary conditions are as follows

At  $z = 0$

$$a_i = a_e = 0$$

At  $z = 1$

$$a_i = a_e = 1 \quad (\text{B-5})$$

In the derivation of Eqs. (B-1), (B-2) and (B-3), it is assumed that

$$\frac{\rho_s \mu}{\rho_s \mu_s} = \frac{T_s \mu}{T_s \mu_s} = b = 1 \quad (\text{B-6})$$

$$\frac{Sc_e}{Sc_i} = \frac{D_i}{D_e} = \sqrt{\frac{M_e}{M_i}} \left( \frac{T_i}{T_e} \right)^2$$

and

$$\frac{K}{D} = \frac{e}{kT}$$

Solutions of the above boundary value problem were obtained numerically mainly for  $(T_i/T_e) = 1$  by Chung (Ref. 2). To avoid excessive numerical complications and to utilize the basic digital computer program used by Chung, we assume that the temperature ratio  $T_i/T_e$  is constant and is equal to the average value within the sheath. Such an approximation should be acceptable for the thin sheaths presently of interest. Solutions of Eqs. (B-1) through (B-3) are obtained for  $A = 3000$  and  $T_i/T_e$  equal to 1, 1/2, 1/3, 1/4, and 1/6, by using a digital computer. Major results are given in Table 1. The reason for choosing this particular value of  $A$  will be explained subsequently.

Although considerable analyses have been made of the high pressure sheaths since the time of Langmuir, most of them lack generality and some of them lack even theoretical soundness. A more detailed evaluation of some of them is given by Su and Lam (Ref. 21). To study the electrical interaction between the plasma considered here and a solid, we must analyze equations of the type given here (Eqs. (1) through (3)) with the proper two-point boundary conditions. The equations are reduced to the type given by Eqs. (B-1) through (B-3) for static plasmas. Only a few of the existing analyses

consider the general solution of these equations for their respective problems. They are: the static electric discharge problem (Allis and Rose, Ref. 22), the plasma-solid interaction at the shock tube end-wall (Sturtevant, Ref. 23), the interaction between a static plasma and a spherical probe (Su and Lam, Ref. 21, and Cohen, Ref. 24), and the Couette and stagnation boundary layer problems (Chung Refs. 2 and 25). Turcotte (Ref. 26) also obtained a solution of the equations similar to Eqs. (B-1) through (B-3) in connection with a shock tube experiment. It is also pointed out here that all these referenced analyses used the same wall boundary conditions as (B-5).

## II. Ambipolar Region

The ambipolar region is defined as that region of the boundary layer where the charge separation is negligible. In this region, therefore,  $m_i = m_e = m$ . The Poisson equation is then extraneous and the two conservation equations describe the region in the manner described below.

Subtracting Eq. (2) from Eq. (1) and integrating once, we obtain at the stagnation region:

$$\rho D_i \frac{\partial m}{\partial y} - \rho K_i E^* m = \rho D_e \frac{\partial m}{\partial y} + \rho K_e E^* m + \gamma_5 \quad (B-7)$$

where  $\gamma_5$  is the constant of integration. By using equations (A-10) and (B-6), Eq. (B-7) can be written in the following form for E:

$$E = \frac{1}{am \left( 1 + \sqrt{\frac{M_i T_e}{M_e T_i}} \right)} \left\{ \sqrt{\frac{1 + \epsilon \beta l^2}{2} \frac{1}{v_s}} \left[ 1 - \sqrt{\frac{M_i}{M_e}} \left( \frac{T_e}{T_i} \right)^2 \right] m' - \frac{Sc_i l}{\mu_s} \gamma_5 \right\} \quad (B-8)$$

where

$$a = \frac{\ell^2}{kT_s/n_{es}e^2} = \left(\frac{\ell}{\Lambda_s}\right)^2 \quad (\text{B-9})$$

$$E = \frac{E^*}{n_{es}e\ell}$$

Here, the integration constant  $\gamma_5$  is important because it determines, for instance, the residual electric field intensity at the boundary layer edge where  $m' = 0$ . As mentioned earlier, the one boundary condition due to the Poisson equation is specified when the current density ratio  $(j_e/j_i)_w$  is specified. We shall, therefore, determine the integration constant  $\gamma_5$  in terms of  $(j_e/j_i)_w$ . Consistent with the preceding assumption of the negligible convection effect in the sheath region, Eqs. (1) and (2) as they approach the sheath edge from the ambipolar region become:

$$\sqrt{\frac{1 + \epsilon}{2} \frac{\beta \ell^2}{v_s}} m' - aEm = J_3 \quad (\text{B-10})$$

$$\sqrt{\frac{1 + \epsilon}{2} \frac{\beta \ell^2}{v_s}} m' + a \frac{T_i}{T_e} Em = J_3 \sqrt{\frac{M_e}{M_i}} \left(\frac{T_i}{T_e}\right)^2 \left(\frac{j_e}{j_i}\right)_w \quad (\text{B-11})$$

where

$$J_3 = -\frac{j_{iw} M_i S_c \ell}{C_{is} \mu_s} \quad (\text{B-12})$$

With a little manipulation of the above equations, we have at the sheath edge:

$$aE_0 m_0 = - \frac{\sqrt{\frac{1+\epsilon}{2}} \frac{\beta l^2}{v_s} \left[ 1 - \sqrt{\frac{M_e}{M_i}} \left(\frac{T_i}{T_e}\right)_0 \left(\frac{j_e}{j_i}\right)_w \right]}{\left(\frac{T_i}{T_e}\right)_0 \left[ 1 + \sqrt{\frac{M_e}{M_i}} \left(\frac{T_i}{T_e}\right)_0 \left(\frac{j_e}{j_i}\right)_w \right]} m'_0 \quad (\text{B-13})$$

After some manipulation, Eqs. (B-8) and (B-13) give:

$$\gamma_5 = \left(\frac{\mu_s}{Sc_1 l}\right) \sqrt{\frac{1+\epsilon}{2}} \frac{\beta l^2}{v_s} \frac{\left[ 1 + \left(\frac{T_e}{T_i}\right)_0 \right]}{\left[ 1 + \sqrt{\frac{M_e}{M_i}} \left(\frac{T_i}{T_e}\right)_0 \left(\frac{j_e}{j_i}\right)_w \right]} \left[ 1 - \left(\frac{j_e}{j_i}\right)_w \right] m'_0 \quad (\text{B-14})$$

Upon eliminating  $\gamma_5$  from Eqs. (B-8) and (B-14), the quantity  $(Em)$  is obtained from equation (B-8) and is substituted into Eq. (1). After the similarity transformation from  $(x, y)$  to  $\eta$ , this equation becomes Eq. (26). The solution of Eq. (26) that satisfies the boundary conditions  $m(\eta_0) = m_0$  and  $m(\infty) = 1$  is shown in Ref. 2 as

$$m = (1 - m_0) \frac{\int_{\eta_0}^{\eta} (f'')^{Sc_a} d\eta}{[4(0.332)]^{Sc_a} \left[ \frac{1}{2(0.332) Sc_a^{1/3} - \eta_0} \right]} + m_0 \quad (\text{B-15})$$

The slight difference in constants between equation (B-15) and its corresponding equation in Ref. 2 is due to the difference in the definition of  $f$  and  $\eta$  of the two analyses. The quantities  $m_0$  and  $\eta_0$  are unknowns and will be determined through the subsequent matching process.

Once the  $m$ -profile is obtained, the electric field intensities in the ambipolar region are obtained from Eq. (30), which is derived by combining Eqs. (B-8) and (B-14).

### III. Matching of the Two Regions

The detailed matching procedure is given in Ref. 2. Here we will only briefly explain the basis upon which the matching is accomplished. In the numerical solution of Eqs. (B-1) through (B-3) it was seen that the region in which the charge separation and the electrical field intensity are pronounced becomes confined to that portion of the sheath region adjacent to the wall as  $A$  is increased (Fig. 4 and also Ref. 2). The charge separation and the electric field intensity become very small in the rest of the region. The solutions for large  $A$  thus produce a sort of ambipolar tail (Fig. 4). The following equations can be derived from Eqs. (B-1) and (B-2) for the ambipolar tail:

$$\alpha = \alpha_i = \alpha_e = 1 - J_1 \frac{\sqrt{\frac{M_e}{M_i}} \left(\frac{T_i}{T_e}\right)^2 \left(\frac{j_e}{j_i}\right)_w + \left(\frac{T_i}{T_e}\right)}{1 + \frac{T_i}{T_e}} (1 - z) \quad (\text{B-16})$$

and

$$H = \frac{J_1}{\alpha A \left(1 - \frac{T_i}{T_e}\right)} \left\{ 2 \frac{\sqrt{\frac{M_e}{M_i}} \left(\frac{T_i}{T_e}\right)^2 \left(\frac{j_e}{j_i}\right)_w + \frac{T_i}{T_e}}{1 + \frac{T_i}{T_e}} - \left[ 1 + \sqrt{\frac{M_e}{M_i}} \left(\frac{T_i}{T_e}\right)^2 \left(\frac{j_e}{j_i}\right)_w \right] \right\} \quad (\text{B-17})$$

The first step in matching the two regions is to obtain a solution of Eqs. (B-1) through (B-3) that has a sufficiently long ambipolar tail for which the ambipolar solutions, Eqs. (B-16) and (B-17), are applicable. It was found that the solutions for  $A = 3000$  produced sufficiently long ambipolar tails for all the cases considered in the present study as shown in Fig. 4. In this tail region, where the solutions of the two regions overlap, the matching is accomplished by requiring that the concentrations and the current densities of the electrons and of the ions, and the electric field intensity be continuous. Such requirements produce the following algebraic equations with the aid of the numerical solutions of Table 1 and Eqs. (B-15) and (30):

$$\eta_0^3 + G_2(J_1 G_3 - 1)\eta_0 - \frac{G_1 G_2 G_3}{\sqrt{2}} J_1 = 0 \quad (\text{B-18})$$

$$m_0 = \frac{1}{J_1 \left[ G_3 \left( \frac{G_1 - \sqrt{2} \eta_0}{\sqrt{2} \eta_0} \right) \right] + 1} \quad (\text{B-19})$$

where

$$G_1 = \frac{1}{0.332 \sqrt{2} S c_a^{1/3}}$$

$$G_2 = \frac{1 + \epsilon}{2} A \left( \frac{\beta l^2}{v_s a} \right) = \frac{1 + \epsilon}{2} A \frac{\beta (\Lambda_s)^2}{v_s} \quad (\text{B-20})$$

$$G_3 = \frac{\frac{T_i}{T_e} + \sqrt{\frac{M_e}{M_i}} \left( \frac{T_i}{T_e} \right)_0^2 \left( \frac{j_e}{j_i} \right)_w}{\left( 1 + \frac{T_i}{T_e} \right)}$$

The temperature ratios  $T_i/T_e$  appearing in Eqs. (B-16) through (B-20), and in Table 1 are the average temperature ratios for the sheath. The solution of Eqs. (B-18) and (B-19) gives  $\eta_0$  and  $m_0$  with which  $m_i$ ,  $m_e$  and  $E$  profiles can be obtained from Eqs. (B-15) and (30) for the ambipolar region. The numerical results for  $\alpha_i$ ,  $\alpha_e$ , and  $H$  obtained for the sheath region can be transformed to  $m_i$ ,  $m_e$  and  $E$  by the use of  $\eta_0$  and  $m_0$ , and the relationships between  $\alpha$  and  $m$ , and  $H$  and  $E$ , respectively. Typical electron and ion concentrations and electric field intensity profiles are shown in Fig. 5. The profiles shown in the figures are those corresponding to the electron temperatures for  $T_{el} = 720$  (Fig. 3).

The potential drop across the boundary layer is obtained by integrating the electric field intensity over the physical thickness of the boundary layer.

Thus

$$\begin{aligned} \frac{e(V_s - V_w)}{kT_s} &= \frac{e(V_0 - V_w)}{kT_s} + \frac{e(V_s - V_0)}{kT_s} \\ &= -A \int_0^1 (\rho_s/\rho) H dz - a \sqrt{\frac{2}{1+\epsilon} \frac{v_s}{\beta l^2}} \int_{\eta_0}^{\infty} (\rho_s/\rho) E d\eta \quad (B-21) \end{aligned}$$

Since  $E$  is given in closed form and  $\rho_s/\rho$  can be obtained from Ref. 5, the second of these integrals may be readily evaluated. However,  $H$  is known only numerically so that the first integral is more difficult. However, Chung has shown (Ref. 2) that

$$\int_0^1 (\rho_s/\rho) H dz \approx \frac{T_w}{T_s} \int_0^1 H dz + 0.59 \left(1 - \frac{T_w}{T_s}\right) \eta_0 \int_0^1 z H dz \quad (B-22)$$



where the two integrals on the right-hand side have been computed for sheath temperature ratios in the span of interest (Table 1).

## REFERENCES

- 1 L. Talbot, "Theory of Stagnation-Point Langmuir Probe," Phys. Fluids 3, 289 (1960).
- 2 P. M. Chung, "Electrical Characteristics of Couette and Stagnation Boundary Layer Flows of Weakly Ionized Gases," TDR-169(3230-12)TN-2, Aerospace Corporation, El Segundo, Calif., (1 October 1962).
- 3 J. A. Fay, "Plasma Boundary Layers," Rept. No. 61-8, Massachusetts Inst. of Tech., Magnetogasdynamics Lab., Cambridge (June 1961); see also ARS Preprint No. 2010-61, American Rocket Society, New York (August 1961).
- 4 H. Petschek and S. Byron, "Approach to Equilibrium Ionization Behind Strong Shock Waves in Argon," Ann. Phys. 1, 270 (1957).
- 5 G. M. Low, "The Compressible Laminar Boundary Layer with Fluid Injection," NACA TN 3404 (1955).
- 6 C. F. Hansen, "Approximations for the Thermodynamic and Transport Properties of High Temperature Air," NASA TR R-50 (1959).
- 7 G. N. Watson, Theory of Bessel Functions, The Macmillan Co., New York (1948).
- 8 Y. L. Luke, Integrals of Bessel Functions, McGraw-Hill Book Co., Inc., New York (1962).
- 9 N. Schwid, "The Asymptotic Forms of the Hermite and Weber Functions," Trans. Amer. Math. Soc. 37, 339 (1935).
- 10 A. Erdelyi, et al., Higher Transcendental Functions, Vol. 2 of The Bateman Manuscript Project, McGraw-Hill Book Co., Inc., New York (1954).
- 11 H. Schlichting, Boundary Layer Theory, McGraw-Hill Book Co., New York (1955).
- 12 L. B. Leob, Basic Processes of Gaseous Electronics, University of California Press, Berkeley (1960).
- 13 D. Bohm, E. H. S. Burhop, and H. S. W. Massey, The Characteristics of Electrical Discharges in Magnetic Fields, McGraw-Hill Book Co., Inc., New York (1955).

- 14 J. A. Fay and F. R. Riddell, "Theory of Stagnation Point Heat Transfer in Dissociated Air," J. Aeronaut. Sci. 25, 73 (1958).
- 15 P. M. Chung and A. D. Anderson, "Heat Transfer Around Blunt Bodies Nonequilibrium Boundary Layers," Proceedings of the 1960 Heat Transfer and Fluid Mechanics Institute, Stanford Univ. Press, Stanford, Calif. (1960), p. 150.
- 16 W. D. Hayes and R. F. Probstein, Hypersonic Flow Theory, Academic Press, Inc., New York (1959).
- 17 S. Chapman and T. G. Cowling, The Mathematical Theory of Non-Uniform Gases, Cambridge University Press, London (1960).
- 18 J. L. Kerrebrock, "Non-Equilibrium Effects on Conductivity and Electrode Heat Transfer in Ionized Gases," CIT TN No. 4, California Inst. of Tech., Pasadena (November 1960).
- 19 L. Spitzer, Jr., Physics of Fully Ionized Gases, Interscience Publishers, Inc., New York (1936).
- 20 L. Talbot, "Note on the Stagnation-Point Langmuir Probe," Phys. Fluids 5, 629 (1962).
- 21 C. H. Su and S. H. Lam, "The Continuum Theory of Spherical Electrostatic Probes," Rep. 605, Princeton Univ., New Jersey (April 1962).
- 22 W. Allis and D. Rose, "The Transition from Free to Ambipolar Diffusion," Phys. Rev. 93, 84 (1954).
- 23 B. Sturtevant, "Diffusion in a Slightly Ionized Gas with Application to Effusion from a Shock Tube," Phys. Fluids 4, 1064 (1961).
- 24 I. M. Cohen, "Asymptotic Theory of Spherical Electrostatic Probes in a Slightly Ionized, Collision-Dominated Gas," MATT-153, Princeton Univ., Princeton, New Jersey (November 1962).
- 25 P. M. Chung, "Langmuir Potential Associated with Couette Flow of Viscous Plasma," Phys. Fluids 5, 1015 (1962).
- 26 D. L. Turcotte and J. Gillespie, "Boundary Layer Resistance and Sheath Potential in a Shock Tube," ARS Preprint No. 2634-62, American Rocket Society, New York (November 1962).

UNCLASSIFIED

Aerospace Corporation, El Segundo, California.  
NONEQUILIBRIUM ELECTRON TEMPERATURE  
EFFECTS IN WEAKLY IONIZED STAGNATION  
BOUNDARY LAYERS, prepared by Paul M. Chung  
and James F. Mullen. 20 May 1963. [78] p.  
incl. illus.  
(Report TDR-169(3230-12)TN-7; SSD-TDR-63-109)  
(Contract AF 04(695)-169) Unclassified report

An electron energy equation is formulated for  
weakly ionized stagnation boundary layers (degree  
of ionization in the order of 0.1 percent or less)  
over highly cooled surfaces. Only the cases of  
moderately negative wall potential with respect to  
the plasma, where the ratio of the electron to ion  
current densities is between about  $10^{-1}$  to  $10^0$ , are  
considered. The equation is simplified by taking  
advantage of the fact that the electron energy equa-  
tion is rather insensitive to the detailed variation  
of the electron concentration profile. A solution of  
(over)

UNCLASSIFIED

UNCLASSIFIED

Aerospace Corporation, El Segundo, California.  
NONEQUILIBRIUM ELECTRON TEMPERATURE  
EFFECTS IN WEAKLY IONIZED STAGNATION  
BOUNDARY LAYERS, prepared by Paul M. Chung  
and James F. Mullen. 20 May 1963. [78] p.  
incl. illus.  
(Report TDR-169(3230-12)TN-7; SSD-TDR-63-109)  
(Contract AF 04(695)-169) Unclassified report

An electron energy equation is formulated for  
weakly ionized stagnation boundary layers (degree  
of ionization in the order of 0.1 percent or less)  
over highly cooled surfaces. Only the cases of  
moderately negative wall potential with respect to  
the plasma, where the ratio of the electron to ion  
current densities is between about  $10^{-1}$  to  $10^0$ , are  
considered. The equation is simplified by taking  
advantage of the fact that the electron energy equa-  
tion is rather insensitive to the detailed variation  
of the electron concentration profile. A solution of

UNCLASSIFIED

UNCLASSIFIED

Aerospace Corporation, El Segundo, California.  
NONEQUILIBRIUM ELECTRON TEMPERATURE  
EFFECTS IN WEAKLY IONIZED STAGNATION  
BOUNDARY LAYERS, prepared by Paul M. Chung  
and James F. Mullen. 20 May 1963. [78] p.  
incl. illus.  
(Report TDR-169(3230-12)TN-7; SSD-TDR-63-109)  
(Contract AF 04(695)-169) Unclassified report

An electron energy equation is formulated for  
weakly ionized stagnation boundary layers (degree  
of ionization in the order of 0.1 percent or less)  
over highly cooled surfaces. Only the cases of  
moderately negative wall potential with respect to  
the plasma, where the ratio of the electron to ion  
current densities is between about  $10^{-1}$  to  $10^0$ , are  
considered. The equation is simplified by taking  
advantage of the fact that the electron energy equa-  
tion is rather insensitive to the detailed variation  
of the electron concentration profile. A solution of  
(over)

UNCLASSIFIED

UNCLASSIFIED

Aerospace Corporation, El Segundo, California.  
NONEQUILIBRIUM ELECTRON TEMPERATURE  
EFFECTS IN WEAKLY IONIZED STAGNATION  
BOUNDARY LAYERS, prepared by Paul M. Chung  
and James F. Mullen. 20 May 1963. [78] p.  
incl. illus.  
(Report TDR-169(3230-12)TN-7; SSD-TDR-63-109)  
(Contract AF 04(695)-169) Unclassified report

An electron energy equation is formulated for  
weakly ionized stagnation boundary layers (degree  
of ionization in the order of 0.1 percent or less)  
over highly cooled surfaces. Only the cases of  
moderately negative wall potential with respect to  
the plasma, where the ratio of the electron to ion  
current densities is between about  $10^{-1}$  to  $10^0$ , are  
considered. The equation is simplified by taking  
advantage of the fact that the electron energy equa-  
tion is rather insensitive to the detailed variation  
of the electron concentration profile. A solution of  
(over)

UNCLASSIFIED

UNCLASSIFIED

the simplified electron energy equation is obtained analytically for the cases where the electron temperatures are not in equilibrium with the neutral gas temperatures. The effects of nonequilibrium electron temperatures on the electrical characteristics of the boundary layer are then analyzed. It was found that the equilibration process of the electron temperatures to the neutral gas temperatures is controlled by the ratio of the characteristic electron energy conduction time to the characteristic temperature equilibration time. The characteristic residence time of electrons has been conventionally used instead of the conduction time. The ion current is found to be dependent on the electron temperature but practically independent of the potential.

UNCLASSIFIED

UNCLASSIFIED

the simplified electron energy equation is obtained analytically for the cases where the electron temperatures are not in equilibrium with the neutral gas temperatures. The effects of nonequilibrium electron temperatures on the electrical characteristics of the boundary layer are then analyzed. It was found that the equilibration process of the electron temperatures to the neutral gas temperatures is controlled by the ratio of the characteristic electron energy conduction time to the characteristic temperature equilibration time. The characteristic residence time of electrons has been conventionally used instead of the conduction time. The ion current is found to be dependent on the electron temperature but practically independent of the potential.

UNCLASSIFIED

UNCLASSIFIED

the simplified electron energy equation is obtained analytically for the cases where the electron temperatures are not in equilibrium with the neutral gas temperatures. The effects of nonequilibrium electron temperatures on the electrical characteristics of the boundary layer are then analyzed. It was found that the equilibration process of the electron temperatures to the neutral gas temperatures is controlled by the ratio of the characteristic electron energy conduction time to the characteristic temperature equilibration time. The characteristic residence time of electrons has been conventionally used instead of the conduction time. The ion current is found to be dependent on the electron temperature but practically independent of the potential.

UNCLASSIFIED

UNCLASSIFIED

the simplified electron energy equation is obtained analytically for the cases where the electron temperatures are not in equilibrium with the neutral gas temperatures. The effects of nonequilibrium electron temperatures on the electrical characteristics of the boundary layer are then analyzed. It was found that the equilibration process of the electron temperatures to the neutral gas temperatures is controlled by the ratio of the characteristic electron energy conduction time to the characteristic temperature equilibration time. The characteristic residence time of electrons has been conventionally used instead of the conduction time. The ion current is found to be dependent on the electron temperature but practically independent of the potential.

UNCLASSIFIED

UNCLASSIFIED

Aerospace Corporation, El Segundo, California.  
NONEQUILIBRIUM ELECTRON TEMPERATURE  
EFFECTS IN WEAKLY IONIZED STAGNATION  
BOUNDARY LAYERS, prepared by Paul M. Chung  
and James F. Mullen. 20 May 1963. [78] p.  
incl. illus.  
(Report TDR-169(3230-12)TN-7; SSD-TDR-63-109)  
(Contract AF 04(695)-169) Unclassified report

An electron energy equation is formulated for weakly ionized stagnation boundary layers (degree of ionization in the order of 0.1 percent or less) over highly cooled surfaces. Only the cases of moderately negative wall potential with respect to the plasma, where the ratio of the electron to ion current densities is between about  $10^{-1}$  to  $10$ , are considered. The equation is simplified by taking advantage of the fact that the electron energy equation is rather insensitive to the detailed variation of the electron concentration profile. A solution of  
(over)

UNCLASSIFIED

UNCLASSIFIED

Aerospace Corporation, El Segundo, California.  
NONEQUILIBRIUM ELECTRON TEMPERATURE  
EFFECTS IN WEAKLY IONIZED STAGNATION  
BOUNDARY LAYERS, prepared by Paul M. Chung  
and James F. Mullen. 20 May 1963. [78] p.  
incl. illus.  
(Report TDR-169(3230-12)TN-7; SSD-TDR-63-109)  
(Contract AF 04(695)-169) Unclassified report

An electron energy equation is formulated for weakly ionized stagnation boundary layers (degree of ionization in the order of 0.1 percent or less) over highly cooled surfaces. Only the cases of moderately negative wall potential with respect to the plasma, where the ratio of the electron to ion current densities is between about  $10^{-1}$  to  $10$ , are considered. The equation is simplified by taking advantage of the fact that the electron energy equation is rather insensitive to the detailed variation of the electron concentration profile. A solution of

UNCLASSIFIED

UNCLASSIFIED

Aerospace Corporation, El Segundo, California.  
NONEQUILIBRIUM ELECTRON TEMPERATURE  
EFFECTS IN WEAKLY IONIZED STAGNATION  
BOUNDARY LAYERS, prepared by Paul M. Chung  
and James F. Mullen. 20 May 1963. [78] p.  
incl. illus.  
(Report TDR-169(3230-12)TN-7; SSD-TDR-63-109)  
(Contract AF 04(695)-169) Unclassified report

An electron energy equation is formulated for weakly ionized stagnation boundary layers (degree of ionization in the order of 0.1 percent or less) over highly cooled surfaces. Only the cases of moderately negative wall potential with respect to the plasma, where the ratio of the electron to ion current densities is between about  $10^{-1}$  to  $10$ , are considered. The equation is simplified by taking advantage of the fact that the electron energy equation is rather insensitive to the detailed variation of the electron concentration profile. A solution of  
(over)

UNCLASSIFIED

UNCLASSIFIED

Aerospace Corporation, El Segundo, California.  
NONEQUILIBRIUM ELECTRON TEMPERATURE  
EFFECTS IN WEAKLY IONIZED STAGNATION  
BOUNDARY LAYERS, prepared by Paul M. Chung  
and James F. Mullen. 20 May 1963. [78] p.  
incl. illus.  
(Report TDR-169(3230-12)TN-7; SSD-TDR-63-109)  
(Contract AF 04(695)-169) Unclassified report

An electron energy equation is formulated for weakly ionized stagnation boundary layers (degree of ionization in the order of 0.1 percent or less) over highly cooled surfaces. Only the cases of moderately negative wall potential with respect to the plasma, where the ratio of the electron to ion current densities is between about  $10^{-1}$  to  $10$ , are considered. The equation is simplified by taking advantage of the fact that the electron energy equation is rather insensitive to the detailed variation of the electron concentration profile. A solution of  
(over)

UNCLASSIFIED

UNCLASSIFIED

the simplified electron energy equation is obtained analytically for the cases where the electron temperatures are not in equilibrium with the neutral gas temperatures. The effects of nonequilibrium electron temperatures on the electrical characteristics of the boundary layer are then analyzed. It was found that the equilibration process of the electron temperatures to the neutral gas temperatures is controlled by the ratio of the characteristic electron energy conduction time to the characteristic temperature equilibration time. The characteristic residence time of electrons has been conventionally used instead of the conduction time. The ion current is found to be dependent on the electron temperature but practically independent of the potential.

UNCLASSIFIED

UNCLASSIFIED

the simplified electron energy equation is obtained analytically for the cases where the electron temperatures are not in equilibrium with the neutral gas temperatures. The effects of nonequilibrium electron temperatures on the electrical characteristics of the boundary layer are then analyzed. It was found that the equilibration process of the electron temperatures to the neutral gas temperatures is controlled by the ratio of the characteristic electron energy conduction time to the characteristic temperature equilibration time. The characteristic residence time of electrons has been conventionally used instead of the conduction time. The ion current is found to be dependent on the electron temperature but practically independent of the potential.

UNCLASSIFIED

UNCLASSIFIED

the simplified electron energy equation is obtained analytically for the cases where the electron temperatures are not in equilibrium with the neutral gas temperatures. The effects of nonequilibrium electron temperatures on the electrical characteristics of the boundary layer are then analyzed. It was found that the equilibration process of the electron temperatures to the neutral gas temperatures is controlled by the ratio of the characteristic electron energy conduction time to the characteristic temperature equilibration time. The characteristic residence time of electrons has been conventionally used instead of the conduction time. The ion current is found to be dependent on the electron temperature but practically independent of the potential.

UNCLASSIFIED

UNCLASSIFIED

the simplified electron energy equation is obtained analytically for the cases where the electron temperatures are not in equilibrium with the neutral gas temperatures. The effects of nonequilibrium electron temperatures on the electrical characteristics of the boundary layer are then analyzed. It was found that the equilibration process of the electron temperatures to the neutral gas temperatures is controlled by the ratio of the characteristic electron energy conduction time to the characteristic temperature equilibration time. The characteristic residence time of electrons has been conventionally used instead of the conduction time. The ion current is found to be dependent on the electron temperature but practically independent of the potential.

UNCLASSIFIED